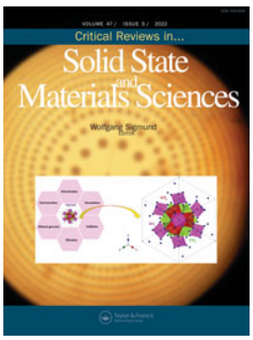

Taylor & Francis
Taylor & Francis Group

Critical Reviews in Solid State and Materials Sciences

ISSN: (Print) (Online) Journal homepage: https://www.tandfonline.com/loi/bsms20

# Current advances in perovskite oxides supported on graphene-based materials as interfacial layers of perovskite solar cells

Samantha Ndlovu, Moses A. Ollengo, Edigar Muchuweni & Vincent O. Nyamori

**To cite this article:** Samantha Ndlovu, Moses A. Ollengo, Edigar Muchuweni & Vincent O. Nyamori (2022): Current advances in perovskite oxides supported on graphene-based materials as interfacial layers of perovskite solar cells, Critical Reviews in Solid State and Materials Sciences, DOI: 10.1080/10408436.2022.2041395

**To link to this article:** https://doi.org/10.1080/10408436.2022.2041395

Published online: 18 Feb 2022.

CRITICAL REVIEWS IN SOLID STATE AND MATERIALS SCIENCES
https://doi.org/10.1080/10408436.2022.2041395

Taylor & Francis
Taylor & Francis Group

REVIEW



# Current advances in perovskite oxides supported on graphene-based materials as interfacial layers of perovskite solar cells

Samantha Ndlovu[a], Moses A. Ollengo[b], Edigar Muchuweni[a]*, and Vincent O. Nyamori[a]

[a]School of Chemistry and Physics, University of KwaZulu-Natal, Durban, South Africa; [b]Chemistry Department, School of Science, Dedan Kimathi University, Nyeri, Kenya

**ABSTRACT**

Perovskite solar cells (PSCs) are emerging efficient photovoltaic devices, with record-high power conversion efficiencies (PCE) of more than 25.5%. However, PSCs exhibit some drawbacks, such as poor stability upon exposure to moisture or humidity, ultraviolet (UV) radiation and heat, which in turn limits the device lifetime and performance. In addition, the introduction of perovskite films comes with associated toxicity, which is a major environmental concern. Furthermore, the application of titanium dioxide ($TiO_2$) as an electron transport layer (ETL) and 2,2′,7,7′-tetrakis[N,N-di(4-methoxyphenyl)amino]-9,9′-spirobifluorene (spiro-OMeTAD) as a hole transport layer (HTL), causes device instability. The wide-bandgap characteristic of $TiO_2$ introduces charge carrier recombination in the ETL, which, in turn, impairs device performance. This is, over and above, the high cost of spiro-OMeTAD, coupled with its multi-step synthetic preparation method. To address the aforementioned shortcomings, approaches, such as modifying the interfacial architecture, have been explored by introducing versatile materials between the charge-collecting electrode and the perovskite active layers. In this regard, perovskite oxides are more appealing due to their wide bandgap and high electron mobility. However, perovskite oxides have limitations due to their agglomeration, which causes short-circuits and leakage current, in addition to their poor charge separation efficiency, surface hydrophilicity and weak visible-light absorption. As a result, nanocomposites of perovskite oxides with carbon-based materials, particularly graphene and its derivatives, have attracted significant research attention due to their exceptional optoelectronic properties, superior stability, and non-toxicity of graphene-based materials. Therefore, this review discusses the recent trends in graphene-based materials, their composites with perovskite oxides, effective ETLs or HTLs of PSCs and the subsequent improvement of photovoltaic performance. In addition, a summary of synthetic routes for perovskite oxides/graphene nanocomposites is presented. This review will foster the advancement of the fabrication of PSCs with improved PCE and stability.

**KEYWORDS**

Graphene; heteroatom-doping; nanocomposites; modification; perovskite oxides; perovskite solar cell

## Table of contents



**CONTACT** Vincent O. Nyamori nyamori@ukzn.ac.za
*On leave from Bindura University of Science Education, Department of Engineering and Physics, Private Bag 1020, Bindura, Zimbabwe

## 1. Introduction

Perovskite solar cells (PSCs) are of great interest due to their low manufacturing cost and high power conversion efficiency (PCE).[1–4] In recent years, the PCE of PSCs has rapidly increased from 3.8% to more than 25.7%.[5–8] The photovoltaic performance and device stability of PSCs can be improved by enhancing the morphology of each functional layer and the device structure, controlling the crystallization of perovskites, and engineering the interfacial structure. One drawback of PSCs is their low efficiency and poor device stability arising from the typical electron transport layer (ETL) and hole transport layer (HTL) materials.[9] To circumvent these issues, the insertion of interfacial layer materials between the ETL or HTL and the perovskite absorber layer can play a significant role in improving device performance and stability.[10] The interfacial layers tune the energy levels between the electrode and perovskite interface, creating an Ohmic contact from a Schottky barrier.[11] This dramatically improves both the light absorption and charge transport while suppressing charge carrier recombination. The other major challenge is moisture, which can be obviated by using hydrophobic graphene-based materials as an interfacial layer leading to improved PSC performance and sustainability.

An effective ETL should not only influence the charge transfer and collection, but also behave as the hole blocking layer to suppress electron-hole ($e^-/h^+$) recombination at the interface.[12] This calls for the exceptional properties of graphene, namely, strong mechanical stability, large specific surface area, and good electrical conductivity.[9] This would enhance charge extraction and charge transport by the ETL, and reduce the recombination rate due to the effective passivation of trap states at the interface, which effectively eliminates J-V hysteresis.[13] Nevertheless, graphene has some limitations, especially when there is restacking of graphene sheets, limiting various properties, such as high surface area and electrical properties.[14] To prevent graphene restacking, metal, metal oxide, and perovskite nanoparticles can be introduced onto the graphene sheets. Also, the wide-bandgap of perovskite oxides can be easily tuned to a low bandgap by incorporating graphene support materials to suppress charge carrier recombination on the device.[15] The interaction of perovskite oxide nanoparticles with the graphene support has a synergistic effect leading to an enhanced surface area and a good electrical conductivity.[16–18] Herein, discussion on hydrophobic graphene-based materials (undoped and doped), as the interfacial layers and support of perovskite oxides, which are resistant to moisture penetration, enhancing device stability, increasing its lifetime and improving its performance, is presented. In addition, different methods of preparing graphene-based materials/perovskite oxide nanocomposites are reviewed.

## 2. Interfacial layers

The main function of the ETL is to transport the photogenerated electrons from the light-harvesting material to the transparent conductive oxide (TCO) while blocking hole transport, thereby suppressing charge carrier recombination and hence improving device efficiency.[19,20] ETLs can also be called a blocking layer, using metal oxides with a wide bandgap.[21] ETLs can help eliminate device hysteresis and enhance electron extraction and transportation.[22] Excellent matching of the energy level of the perovskite absorbing layer with the conduction band of the ETL leads to good electron extraction efficiency and low charge transfer resistance.[23] The most commonly used and successful type of PSC device architecture is a fluorine-doped tin oxide (FTO)/HTL/perovskite-harvester/ETL/indium tin oxide (ITO) either as mesoscopic or

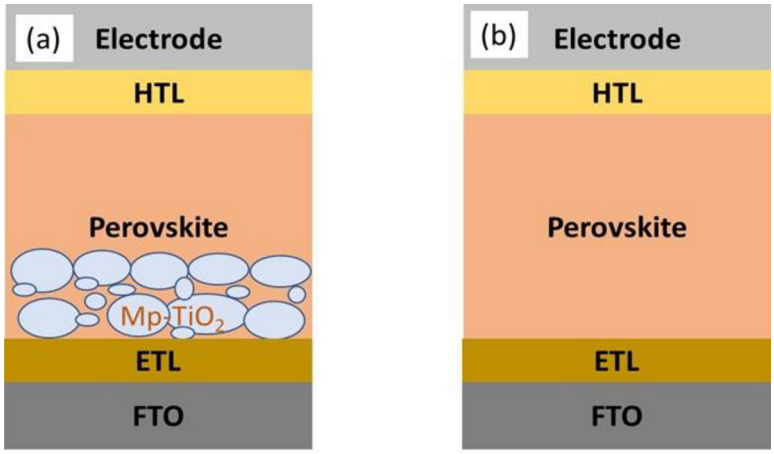


**Figure 1.** Structure diagram of (a) mesoscopic and (b) planar perovskite solar cell.

planar (Figure 1), in which electrons are injected from the perovskite harvester to an ETL, and finally collected by FTO.[24,25] The most common ETL in PSCs is titanium dioxide ($TiO_2$) due to its low cost. However, $TiO_2$ has a wide bandgap, which increases the recombination rate and reduces the electrical conductivity due to defects on $Ti^{3+}$ and oxygen vacancies; hence, reducing the PCE.[9] Zinc oxide (ZnO), as an alternative ETL, demonstrates better electron mobility than $TiO_2$.[9] However, ZnO possesses high charge recombination and chemical instability when interacting with the perovskite absorber.[9]

On the other hand, HTLs play a vital role by preventing direct contact between the metal electrode and perovskite layer, which suppresses the recombination of electrons and holes by transporting holes to a specific back contact metal electrode while blocking any electron transfer to the anode.[26] So far, organic HTLs, such as poly(3-hexylthiophene) (P3HT), poly(triarylamine) (PTAA) and 2,2′,7,7′-tetrakis[N,N-di(4-methoxyphenyl)amino]-9,9′-spirobifluorene (spiro-OMeTAD), are mostly used for fabricating high-performance PSCs.[27] Among these, spiro-OMeTAD has shown a tremendous increase in PCE from 3.8 to 25.7%.[28–32] However, the high cost limits the use of spiro-OMeTAD.[33] Also, poly(3,4-ethylenedioxythiophene):poly(styrenesulfonate) (PEDOT:PSS) exhibits poor long-term stability due to its acidic and hygroscopic nature.[34] In addition, PTAA and P3HT have relatively poor stability due to their inability to prevent moisture ingress.[35] Therefore, alternative interfacial layers have gained significant research interest to overcome the aforementioned disadvantages. In particular, graphene-based materials offer distinct advantages of low cost, excellent stability and unique optoelectronic properties.

## 3. Stability of perovskite solar cells

Researchers have invested significant efforts to improve the interfacial engineering of PSCs to enhance not only the PCE but also the stability of PSCs.[36] This has been achieved through the use of a variety of transport layers, selective charge collection electrodes and active layers. Nevertheless, PSCs are vulnerable to a number of factors, such as temperature, UV radiation, oxygen and moisture, which lead to degradation, as illustrated in Figure 2(a).[37]

The instability of PSCs is mainly influenced by the degradation of the interfacial layers and the degradation of the perovskite itself.[38] The degradation of the perovskite has been a critical issue, especially when applying $CH_3NH_3I$ and $PbI_2$, which decompose in a high humidity environment, resulting in poor instability in light due to their hydrophilic nature.[39] Another concern is the usage of organic charge transport layers that can be easily influenced by atmospheric water and oxygen, which can contribute to the degradation of PSC devices.[40] Also, the metal electrodes, such as Al and Ag, can easily react with perovskite absorbers when they are in direct contact.[40] However, an electrode, such as Au, cannot undergo any corrosion, but this metal is too costly for large-scale commercialization.[41] Hence, the challenge is to overcome the poor stability of PSCs by using a controlled environment and highly stable materials to improve the stability in severe conditions, such as high temperature, high humidity and UV illumination, as shown in Figure 2(b). At this point, we present a review of graphene-based materials with perovskite oxides that can be used to protect the PSC device when exposed to atmospheric moisture while maintaining the good stability of the device.

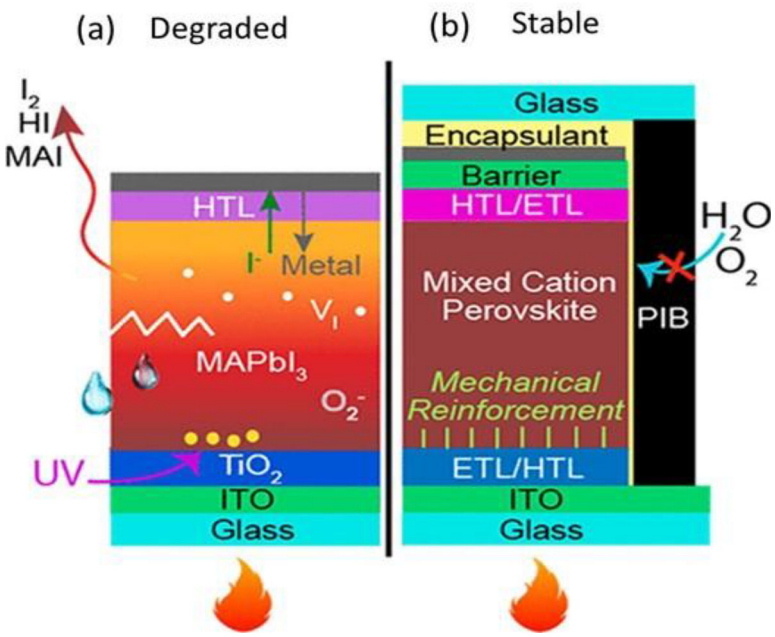


**Figure 2.** The (a) degraded and (b) stable PSCs. Adapted with permission.[35] Copyright 2019, American Chemical Society.

## 4 Perovskite oxides

Perovskite oxide materials play a significant role in the emerging field of photovoltaics because of their potential to improve the PCE of solar cells.[42] Perovskite oxides exhibit a cubic structure, with the general formula of $ABO_3$, where the A-site ion is usually a rare-earth element or an alkaline earth metal situated at the center of the lattice, the B-site ion is a transition metal positioned at the lattice corners.[43,44] Perovskite oxides have been applied in solar cells as the hole-transporter,[45] sensitizers,[46] and the electron- and hole-transporter.[47] They can possess an energy bandgap in the range from 1.4 to 3.8 eV, which allows these materials to be useful as interfacial layers.[48] Any distortion formed on the nanostructure of perovskite oxides can influence different physical properties, such as the dielectric, optical, magnetic and electronic properties.[48] The size and structure of perovskite oxides play a substantial role in tuning the physical and chemical properties, which subsequently influence their various applications, e.g., in photocatalysis,[49] light-emitting diodes,[50] electrochemical devices[51] and solar energy conversion.[42]

The preparation method is a key factor that contributes to a good structure and superior physicochemical properties. Some of the methods used to prepare perovskite oxides are sol-gel,[52,53] combustion synthesis,[54] sonochemical,[55] microemulsion,[56] electrospinning,[57] and co-precipitation.[58] For perovskite oxides at the nanometer scale, the agglomeration has been considered a serious concern that can lead to short-circuits and leakage current.[52] Agglomeration in perovskite oxides can cause limited transparency and poor performance in optoelectronic devices.[52] Also, perovskite oxides have drawbacks, such as poor charge separation efficiency, surface hydrophilicity and weak visible-light absorption.[59,60] To circumvent these issues, the introduction of graphene-based materials into perovskite oxides as the support can prevent agglomeration and also suppress the charge recombination rate, which favors charge transport by forming a suitable band alignment.[61] Also, the addition of graphene-based materials into perovskite oxides can act as a highly conductive support and provides a good interfacial contact, which increases the electrical conductivity.[62]

## 5 Graphene-based materials

The primary concern for commercial applications of PSC devices is moisture and stability due to the use of volatile components.[63] Carbon-based materials can assist in discouraging humidity penetration due to their hydrophobic nature. Additionally, the interface architecture can also act as the buffer layer to further prevent metal-atom penetration onto the perovskite harvester.[64] Various interfacial materials, such as water-resistant metal nanostructures, carbon materials, and graphene-materials, such as graphene oxide (GO), reduced graphene oxide (RGO),[65] graphene quantum dots (GQDs),[66] graphene nanosheets (GNSs),[67] and graphene nanoribbons (GNRs),[68] have been used due to their better stability, and efficiency.[69]

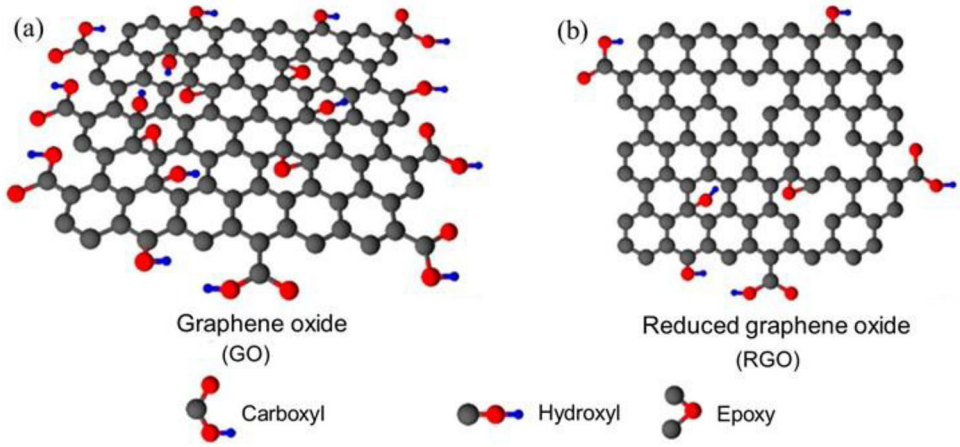


**Figure 3.** Illustration of (a) graphene oxide and (b) reduced graphene oxide sheet. Adapted with permission.[73] Copyright 2019, Nanomaterials.

Graphene-based materials can be synthesized through either covalent or non-covalent, doping polymers and chemical functionalization.[70] Any of these methods can create different graphene derivatives with a unique oxidation level. Graphene is one of the most attractive materials since it is a 2 D single layer of $sp^2$-hybridized carbon atoms, whereby the $sp^2$-hybridization is formed from the $\sigma$-bonds (in-plane) and pi-bonds (out-plane).[71,72] The formation of graphene, as multilayer graphene (MLG) achieves higher charge carrier mobilities of $\sim$60000 $cm^2$ $V^{-1}$ $s^{-1}$ at 4 K, and $\sim$15000 $cm^2$ $V^{-1}$ $s^{-1}$ at 300 K.[73] On the other hand, few-layer graphene (FLG) can have relatively low charge carrier mobilities of up to 10000 $cm^2$ $V^{-1}$ $s^{-1}$.[73] In addition, FLG has displayed excellent optical transparency of up to 95% in the visible range, with high charge carrier mobility, thus, graphene-based materials are excellent candidates for PSC fabrication.[74]

### 5.1. Graphene oxide and reduced graphene oxide

GO is formed from covalent carbon-oxygen (C-O) bonds, making it an insulator with a wide bandgap due to a mixture of $sp^2$ and $sp^3$ hybridization.[75] GO has major functional groups, such as carbonyl (-C-OH) and carboxyl (-COOH) on the $sp^2$-hybridized carbons, and hydroxyl (-OH), and epoxide (C-O-C) situated on the $sp^3$-hybridized carbons, as shown in Figure 3(a)[75]. The oxygenated functional groups allow for ease of chemical functionalization and have hydrophilic characteristics that make GO to be easily exfoliated in water.[75] Thus, GO can be chemically functionalized with other materials, such as hybrid organic and inorganic materials, to form novel nanocomposites.[76] Nevertheless, the oxygen functional groups tend to reduce the intrinsic electrical and thermal conductivity and can be easily removed through chemical treatment or high-temperature thermal annealing, resulting in a semi-metallic state.[76,77]

RGO is a semi-metallic material obtained from chemically exfoliated GO, either from the chemical or thermal removal of oxygenated functional groups, as revealed in Figure 3(b)[77]. The chemical method uses corrosive reagents such as sulfuric acid, which are not considered green, while the thermal method uses heat to break down weak van der Waals forces of attraction between the sheets.[77] Although these methods can result in some oxygenated functional groups remaining, these can be utilized to incorporate perovskite oxides or support other nanoparticles, enhancing chemical stability, electrical conductivity and forming a high surface area material.[78]

### 5.2. Graphene quantum dots

GQDs have a zero-dimensional structure (Figure 4) containing $sp^2$-$sp^{[2]}$ hybridized carbon bonds that impart stable structural and excellent optical properties.[79] GQDs can be prepared via a top-down approach, i.e., from small fragments of graphene sheet layers.[80] GQDs show quantum confinement, more abundant active sites, and are comparable in size to biomolecules.[81] They can contain various functional moieties, which allows for complex bandgap structures and catalytic abilities.[81] Water molecules and oxygen can be adsorbed by GQDs to create defects on the energy level toward the highest occupied molecular orbital (HOMO) level, as revealed by Shin et al.[79] They observed that the addition of a GQD layer could reduce charge carrier recombination, and increase the stability of a PSC relative to PEDOT:TSS alone. Pang

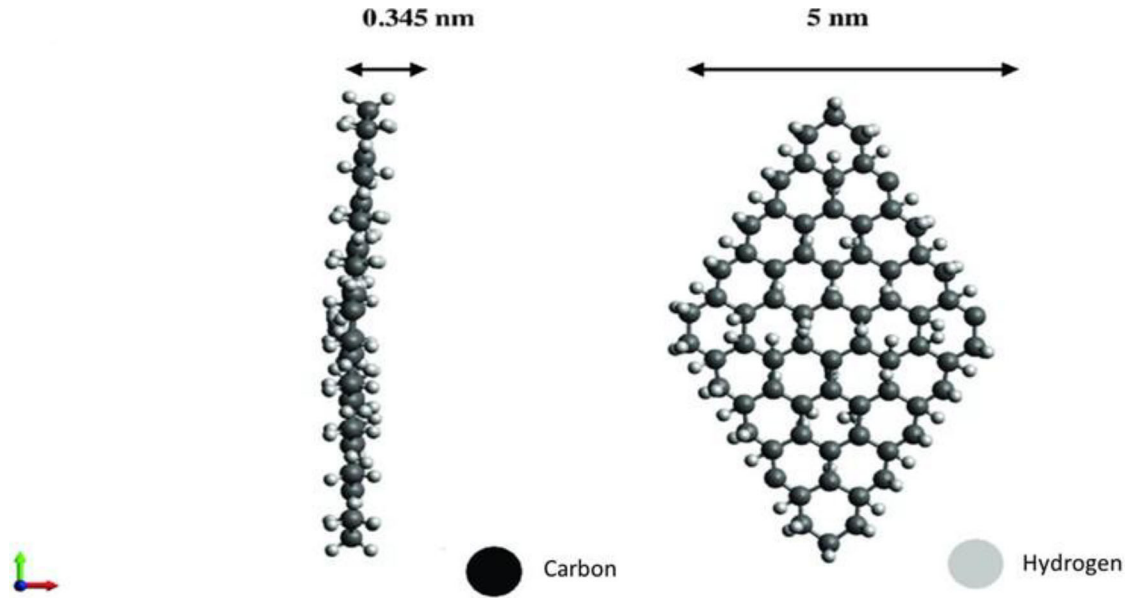


**Figure 4.** Molecular diagram of graphene quantum dots (GQDs). Adapted with permission.[79] Copyright 2020, Elsevier.

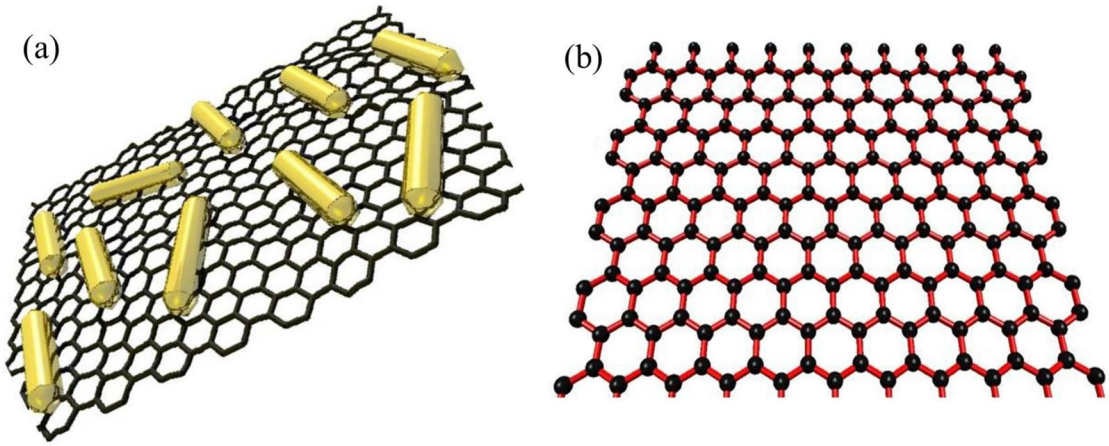


**Figure 5.** (a) Illustration of graphene nanorods. Adapted with permission.82 Copyright 2011, Royal Society of Chemistry. (b) Illustration of graphene nanosheets. Adapted with permission.83 Copyright 2017, IGI global.

et al.[82] synthesized GQDs decorated by tin(IV) oxide ($SnO_2$) as the ETL of a PSC and compared the result with $SnO_2$. They observed the suppression of charge carrier recombination and enhanced electron extraction. GQDs, as interfacial layers, can form an excellent matching energy level, which can further suppress $e^-$/$h^+$ recombination rate, to improve device performance.

### 5.3. Graphene nanorods and graphene nanosheets

GNRs are made up of a one-dimensional graphene sheet from elongated strips of graphene layers with an ultra-thin width of <50 nm, as shown in Figure 5(a).[83] GNRs can be either metallic or nonmetallic. GNSs form two-dimensional graphene nanosheets (Figure 5(b)),[84] that differ from regular graphene sheets, based on the quasi-periodic nanoholes compared to GNRs. This makes GNSs to have more active sites, leading to higher electrocatalytic activities and faster electron transport.[84] All these graphene-based materials have exceptional properties, such as high optical transmittance in the visible region, large surface area, high electrical conductivity and better stability.

## 6. Modifications of graphene-based materials

In this section, various modifications carried out to improve the optoelectronic properties of graphene-based materials are presented. Modifications, such as heteroatom-doping of graphene and formation of


**Figure 6.** The formation of boron-doped graphene (BRG) from graphene oxide (GO). Adapted with permission.[87] Copyright 2018, Elsevier.

perovskite oxide/graphene nanocomposites, will be systematically discussed.

### 6.1. Heteroatom-doping

The chemical modification of graphene alters its electronic properties, such as the Fermi level, bandgap, thermal stability, charge transport, spin density, magnetic, electrical, and optical properties,[85] due to the electron modulation caused by the difference in electronegativities during doping of heteroatoms into the graphene sheet.

#### 6.1.1. Boron doping

Boron (B), $2s^2 2p^1$, is a neighbor element of C, $2s^2 2p^2$, on the periodic table.[86] Boron can easily substitute a carbon atom in the GO lattice due to size compatibility, as illustrated in Figure 6. B-doping results in $sp^2$ hybridization that is electron-deficient (p-type), with charge polarization between neighboring carbons. Furthermore, the C-C (∼1.42 Ð) bond is shorter than the B-C bond (∼1.50 Ð); thus, inducing intrabond strain.[88] The electron-deficient nature of B imposes p-type and p-doping effects, thereby decreasing the Fermi level, and increasing the doping level.[89] The incorporation of B onto the graphene lattice allows it to assemble at the interstitial sites, which increases the bond length,[90] and hence improves the conductivity and PCE of the device. Ideally, doping B onto graphene can increase the work function of the graphite sheet via the replacement of C with a B atom. Li et al.[87] used the chemical vapor deposition (CVD) to synthesize B-doped graphene using boron hydride as a boron source and obtained an enhanced PCE of 3.4% when a p-type semiconductor material was used.

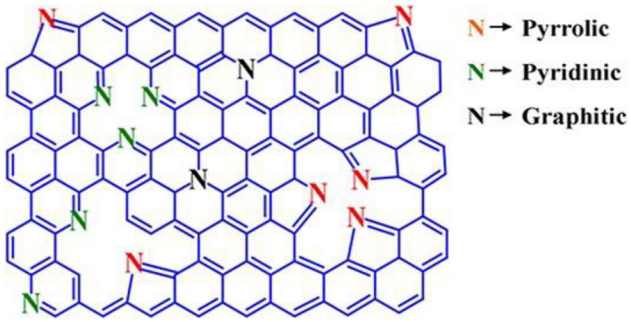


**Figure 7.** Schematic diagram of the different configurations of N in doped graphene sheet. Adapted with permission.96 Copyright 2016, IntechOpen.

They also improved the conductivity and work function of B-doped graphene by using a nitric acid surface treatment.

#### 6.1.2. Nitrogen doping

Nitrogen (N), $1s^2 2s^2 sp^3$, is an immediate neighbor element of C in the periodic table of elements and is electron-rich in nature (n-type). N-doping can exist in three configurations: *viz.,* pyridinic, pyrrolic, and graphitic, as shown in Figure 7. Zhang et al.[91] synthesized amino-functionalized graphene and characterized the materials with X-ray photoelectron spectroscopy (XPS). The graphiticC and pyridinic N exert marginal intrabond strain due to the comparable bond lengths of C-C (1.42 Ð) and C-N (1.41 Ð). However, the introduction of N improves the work function of graphene as a result of the nonbonding electrons. Studies have shown that N-doped graphene can enhance electrocatalytic activities and electron transfer properties due to the additional lone pairs of electrons that create defects on the graphene-material

matrix.[92–94] Zhu et al.[95] synthesized N-doped graphene using a one-step fast pyrolysis method and achieved an improved PCE of 10.3% when the material was used as a counter electrode in PSC. They observed that N-doping increased the electrical conductivity and charge extraction capability.

#### 6.1.3. Phosphorus doping

Phosphorus (P), $3p^2 3p^3$, forms a pyramidal bonding configuration with three carbon atoms, as shown in Figure 8. P-doping creates more structural distortion, transforming the $sp^2$ hybridized carbon to the $sp^3$ state. It is well known that P is an n-type dopant, which enhances the charge extraction efficiency, potentially reducing charge carrier recombination at the perovskite interface.[96] The extra electron causes a localized state, and a nonzero magnetic moment is obtained due to the charge transfer from P to graphene.[96]

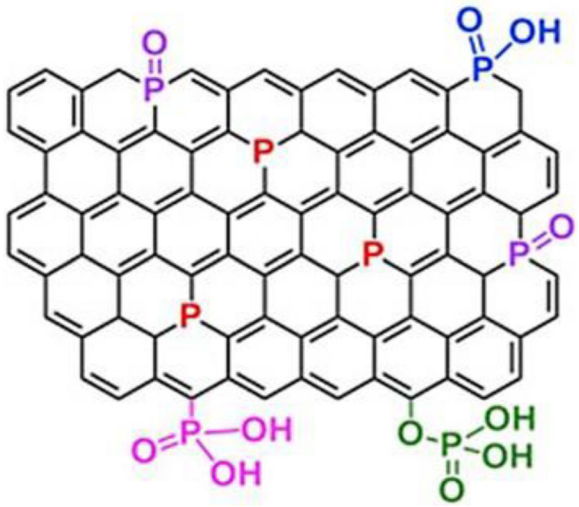


**Figure 8.** Different configurations of P species on RGO sheet, showing C (gray), P (blue) and O (red). Adapted with permission.97 Copyright 2017, Elsevier.

#### 6.1.4. Sulfur doping

The sulfur-carbon (S-C) bond length is longer (1.78 Ð) than the C-C bond.[97] Consequently, S-doping of graphene has drawbacks because of the size and the binding behavior of the S atom, as shown in Figure 9. Unlike N, B and P, there is no polarization or charge transfer on the C-S bond due to the same electronegativity of C (2.55) and S (2.58). The synthesis of S-doped graphene is even more difficult due to the considerable energy of formation required. Thus, limited attempts have been made; for instance, S-RGO was used as the counter electrode in a dye-sensitized solar cell, and an efficiency of 4.2% was obtained, as reported by Luo et al.[98] Li et al.[98] employed S-doping onto GQDs by using a hydrothermal method. XPS revealed two configurations of S on the GQDs: oxide-S and thiophene-S.[99] The S-bonding can assist in altering different physicochemical properties. S-doping provides an extra electronic transition and an additional energy level ($\pi \rightarrow \pi^*$) on carbon.[99] In this regard, heteroatom-doping can reduce charge carrier recombination, increase grain size, enhance optical properties, and improve the morphology of graphene materials, resulting in enhanced device performance.

### 6.2. Graphene hybrid materials

#### 6.2.1. Perovskite oxide ($ABO_3$)/graphene nanocomposites

In order to improve the photocatalytic performance of graphene, it has been fabricated into composites with other materials.[100] For instance, perovskite oxides are known to enhance the catalytic performance, mechanical flexibility, dielectric properties and ductility of materials, as well as reduce electron-hole recombination.[101] Graphene materials have attractive physical and chemical properties that could provide a

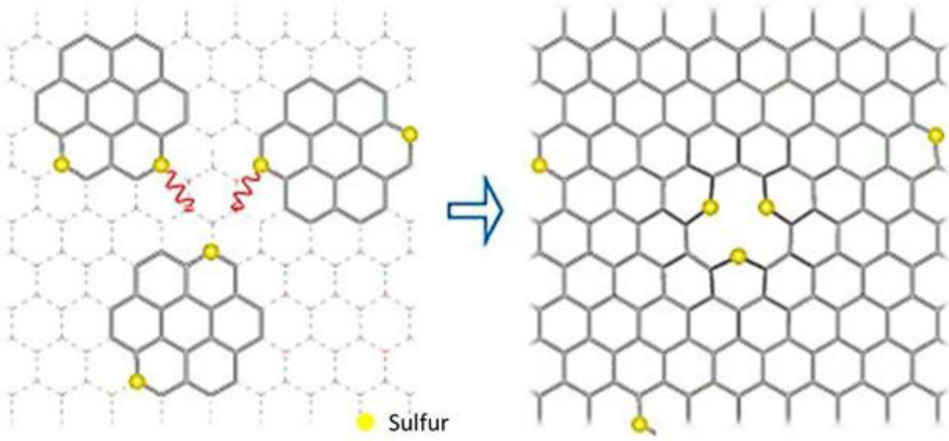


**Figure 9.** The sulfur doping of graphene. Adapted with permission.101 Copyright 2017, Elsevier.

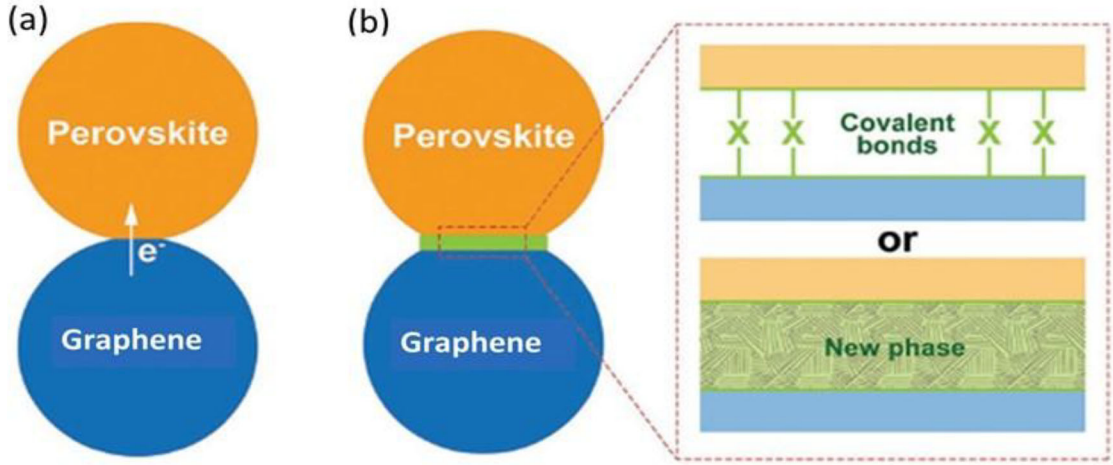


**Figure 10.** The general representation of synergistic effect between graphene and perovskite atoms, as (a) ligand effect and (b) bond formation of interfacial heterostructures. Adapted with permission.103 Copyright 2017, John Wiley and Sons.

synergistic effect (Figure 10) to perovskite oxides and provide an electrochemically active center with graphene, serving as a support.[102] Both graphene and perovskite atoms can form the interfacial covalent bond, which can act as the electron transfer connector between the two and can improve the catalytic performance of the composites.[102] Similarly, the ligand effect on the interface can alter the electronic structure to facilitate electron transfer.[103]

Perovskite oxides such as $BiFeO_3$ have a good narrow bandgap of about 1.8 to 2.2 eV, making them suitable for solar cell applications.[61,104] The combination of perovskite oxides and graphene-based materials enhances the electron-donating capability and reduces the recombination of the photogenerated charges. Correspondingly, the addition of graphene to a perovskite oxide acts as a highly conductive interfacial layer support that promotes electrical conductivity.[60,62]

Sun et al.[105] synthesized a superparamagnetic iron sillenite ($Bi_{25}FeO_{40}$)-graphene composite for use as a photocatalyst through a one-step hydrothermal method. A larger surface area of $S_{BET} = 59.0\,m^2\ g^{-1}$ was obtained for the $Bi_{25}FeO_{40}$-graphene composite compared with bismuth ferrite ($BiFeO_3$) of $S_{BET} = 3.6\,m^2\ g^{-1}$.[106] The high surface area was able to improve the adsorption sites and reduce $e^-/h^+$ recombination. Fe-based perovskite oxides absorb visible light due to the presence of Fe, which can work well with solar cells because of the abundance of visible light in the solar spectrum.[105]

Nayak et al.[107] reported the sol-gel synthesis of a $BiFeO_3$-graphene nanocomposite calcined at 500 °C. They obtained $BiFeO_3$ nanoparticles with a large $100-200\,nm$ diameter on a graphene sheet. However, they observed the presence of impurity phases such as $Bi_{25}FeO_{40}$. The disadvantage of the sol-gel method is the post-treatment of the products and the formation of by-products.[108] Hu et al.[109] reported the synthesis of a graphene-$Bi_2Fe_4O_9$ composite using a one-pot co-precipitation method at 95 °C. Using Fourier-transform infrared spectroscopy (FTIR) analysis, they observed the composite to be chemically bonded through Bi-O-C or Fe-O-C bonds. The co-precipitation method assisted in producing small particle sizes of 5 nm with enhanced physicochemical properties, although the reaction was multistep.[110] Nevertheless, co-precipitation is the technique mostly used to produce controlled sizes of nanoparticles of less than 10 nm.[111]

Meanwhile, Cao et al.[112] utilized an *in situ* solvothermal method to synthesize cobalt tin oxide ($CoSnO_3$)/graphene (space group *Pn3m*) calcined at 300 °C. This method gave rise to impurities, such as $CoSnO_4$ and $SnO_2$, instead of pure $CoSnO_3$, resulting from side-reactions. Finally, Li et al.[113] reported the simple synthesis of RGO-$BiFeO_3$, as illustrated in Figure 11. Their study revealed the change of energy bandgap from 3.2 eV, for $BiFeO_3$, to 2.5 eV, for RGO-$BiFeO_3$, which was lowered by introducing RGO. They obtained enhanced magnetic and optical properties, thus, allowing this nanocomposite to be suitable for use as PSC interfacial layers.

In this case, smaller particle sizes improved the surface area and charge carrier transportation capability as a desired characteristic for interfacial layers. Furthermore, introducing graphene into perovskite oxides can prevent agglomeration and suppress the recombination rate, which favors charge transport by forming a suitable band alignment.

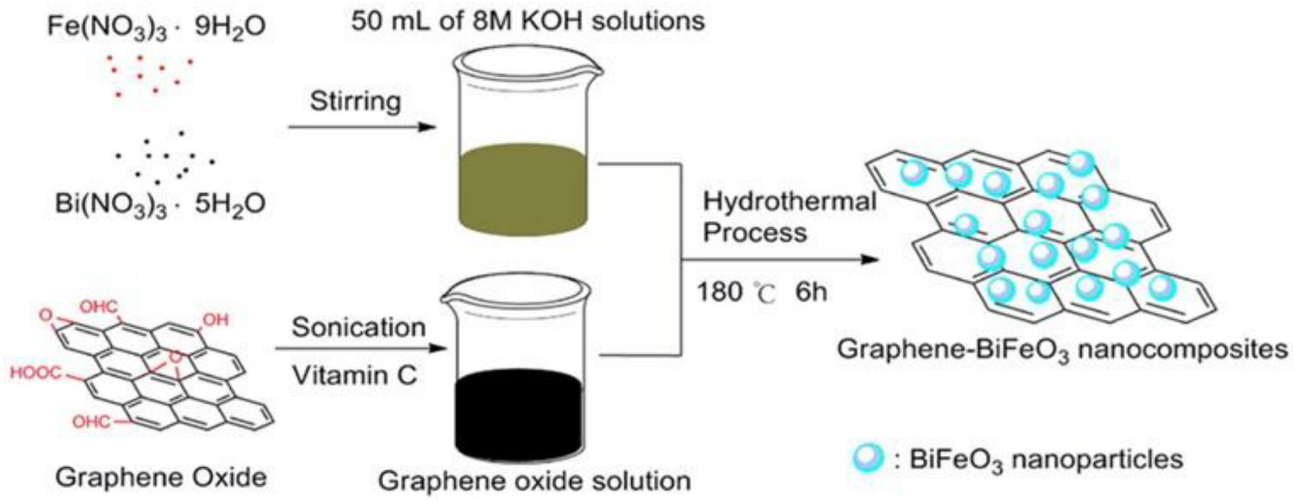


**Figure 11.** The simple mechanism of preparing RGO/$BiFeO_3$. Adapted with permission.114 Copyright 2013, Elsevier.

#### 6.2.2. Perovskite oxides ($AB_2X_4$)/graphene nanocomposites

Several researchers have prepared composites of graphene and spinels that exhibit better photocatalytic activities; for example, Lu et al.[114] fabricated a $ZnFe_2O_4$-graphene composite using a one-pot solvothermal reaction, and GO was automatically reduced to graphene. They obtained $ZnFeO_4$ with average particle sizes of 200 nm. The excellent uniform distribution of $ZnFeO_4$ nanoparticles onto the graphene sheets enhanced catalytic efficiency. Evidently, the solvothermal technique has been found to be a suitable low-temperature synthetic route that yields a good distribution of nanoparticles on the support, such as graphene.[115]

Li et al.[116] demonstrated the formation of cobalt ferrite ($CoFe_2O_4$)-functionalized graphene by employing a hydrothermal reaction, as illustrated in Figure 12. They observed a strong interaction of the inorganic salts, i.e., $Fe^{3+}$ and $Co^{3+}$ with –OH, and functionalized graphene during the reaction process. They noted that graphene absorbs the intermediate product, forming graphene sheets with oxygen functionalities. Wang et al.[117] reported the synthesis of RGO-$ZnFe_2O_4$ nanohybrids using a one-pot hydrothermal synthesis method. The GO was prepared by the modified Hummers method,[118] and zinc nitrate hexahydrate ($Zn(NO_2)_3{\bullet}6H_2O$), and iron(III) nitrate nonahydrate ($Fe(NO_3)_3{\bullet}9H_2O$) were used as the precursor materials. They concluded that the RGO-$ZnFe_2O_4$ nanocomposite has more effective active sites that increase the catalytic activity of the material than $ZnFe_2O_4$ alone. In essence, the hydrothermal method is one of the techniques that require a low temperature for a synthesis with good reproducibility.[113]

The formation of perovskite oxides/graphene nanocomposites can be characterized using various techniques. The obtained nanocomposites can be dependent on the morphology, chemical composition and particle sizes. When Lu et al.[114] prepared $ZnFe_2O_4$-graphene using a one-pot solvothermal reaction, they examined the composition and crystalline nature of the nanocomposites using powder X-ray Diffraction (XRD). They further observed a shift in the diffraction angle from 10.6° (002) to 21.2° (002), as well as the conversion of GO to crystalline graphene after the deposition of $ZnFe_2O_4$ particles onto the graphene surface. On using scanning electron microscopy (SEM) and transmission electron microscopy (TEM) to analyze the morphology and microstructure of $CoFe_2O_4$-functionalized graphene sheet nanocomposites, Li et al.[116] observed the $CoFe_2O_4$ nanoparticles to be well distributed on the graphene sheets with particles sizes of $10-40$ nm, which led to a high surface area. In this case, graphene-based materials have been considered as the best support for perovskite oxides and metal nanoparticles.

## 7. Application of graphene-based materials and perovskite oxides as interfacial layers of PSCs

Graphene-based materials have been used as interfacial layer material in solar cells. This section highlights specific graphene materials incorporated into perovskite solar cells.

### 7.1. Graphene nanocomposites

Several authors have demonstrated that different derivatives of graphene materials can enhance the

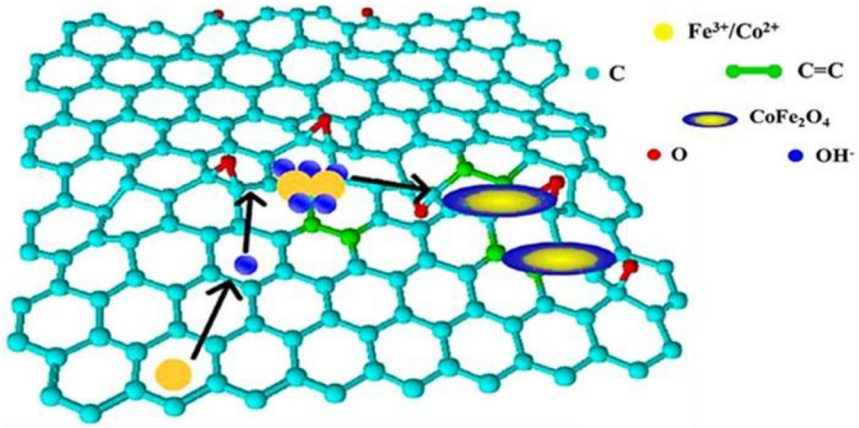


**Figure 12.** Schematic diagram of the CoFe2O4/functionalized graphene mechanism. Adapted with permission.117 Copyright 2011, Elsevier.

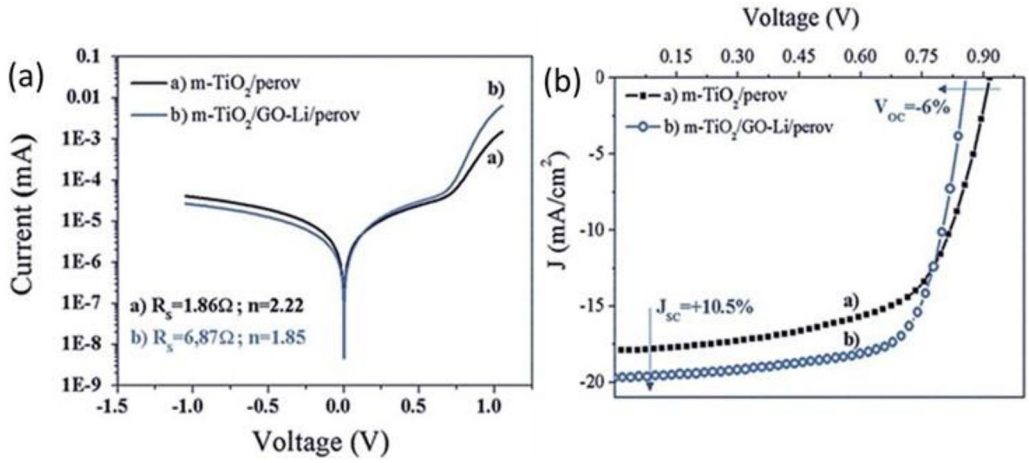


**Figure 13.** A typical photovoltaic characteristics, i.e., (a) dark I-V characteristics and (b) J-V curves of the device with GO. Adapted with permission.122 Copyright 2016, John Wiley and Sons.

stability and performance of PSCs.[75,119,120] Agresti et al.[121] designed a PSC with GO-lithium (Li) as an interlayer, situated between the perovskite harvester and $TiO_2$. They observed an improved device efficiency due to the enhanced electron extraction and injection capabilities of their device. The addition of Li to GO promoted the transfer of charges from Li to GO, resulting in a Fermi level shift, and a smaller work function. The results obtained revealed the enhancement in fill factor (FF) and on the short-circuit current density ($J_{sc}$) with reduced hysteresis, as shown in Figure 13(a) and (b).

In an attempt to suppress charge carrier recombination, Nouri et al.[122] prepared PSCs with Li-GO/$TiO_x$ as the ETL, and GO/nickel oxide (NiO) as the HTL, and they were able to obtain PCEs of up to 11.2%. They observed that the presence of graphene derivatives, on both sides as interfacial layers of the device, could protect the perovskite layer from humid conditions and exposure to moisture. A similar trend was observed by Sahin et al.,[123] when they used modified-GO as the buffer layer to assist in reducing charge carrier recombination in their device. GO as the buffer layer has been observed to decrease current leakage and reduce charge recombination, which subsequently improves the $J_{sc}$ and PCE of PSCs. Mahmoudi et al.[124] prepared perovskite/Ag-RGO as an ETL for PSC devices. They observed an enhancement in charge transport upon the introduction of graphene due to its excellent electrical conductivity. Wang et al.[125] also prepared a graphene-$TiO_2$ nanocomposite as an ETL, and their device showed improved FF and $J_{sc}$, with a PCE of about 15.6%. They noted that graphene forms excellent electrical contacts with $TiO_2$, while maintaining a high electrical conductivity, allowing graphene to serve as an excellent electron acceptor and collection material. Shen et al.[126] prepared a device using GQDs/$TiO_2$ with a PCE of 20.5%. This resulted from the excellent electron extraction, reduced series resistance and high $J_{sc}$.

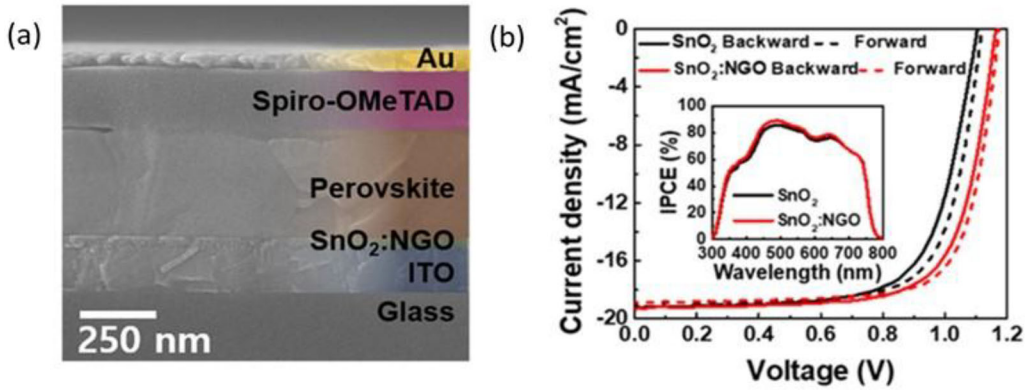


**Figure 14.** The (a) SEM cross-section of the prepared PSC with SnO2:NGO and (b) J-V curves with the best performing nanocomposites. Adapted with permission.146 Copyright 2020, American Chemical Society.

Xie et al.[127] fabricated a device with $SnO_2$-GQD and obtained an average PCE of 20.2%. Good performance on the device was obtained as a result of a decrease in the recombination rate and efficient electron transportation with reduced hysteresis. GQDs provide segregated trap sites when incorporated with $SnO_2$, thus, act as localized reservoirs that decrease the recombination rate and enhance electron mobility.

Redondo-Obispo et al.[128] fabricated inverted PSCs by doping PEDOT:PSS with graphene. They demonstrated that the incorporation of graphene into PEDOT:PSS helps improve the electrical conductivity ten times without affecting the optical transmittance. In addition, spiro-OMeTAD is a volatile material, making devices that use it easily exposed to moisture. Yeo et al.[129] applied RGO-spiro-OMeTAD as the HTL for PSCs, and obtained an enhanced PCE of 10.8%. They observed that the presence of RGO improved the device performance and stability because of the enhanced electrical conductivity and low recombination rate of the photogenerated charges, coupled with the excellent stability of RGO. In this regard, graphene-based materials as an interfacial layer can help to improve the stability, while lowering the charge carrier recombination rate and further improving the $J_{sc,}$ which improves the device performance. A summary of the reported applications of graphene-based materials as interfacial layers in PSCs is shown in Table 1.

### 7.2. Heteroatom-doped graphene nanocomposites

Heteroatom doping can have an effect on altering the electronic properties of graphene. Hong et al.[130] fabricated a PSC with $SnO_2$-nitrogen-doped graphene oxide (NGO) as an ETL, as illustrated in Figure 14(a). They obtained a high PCE of 16.5% with an enhanced $V_{oc}$ and $J_{sc}$, when compared with a PCE of 15.4% obtained with $SnO_2$ alone, as shown in Figure 14(b). The high performance of their devices was ascribed to the low recombination rate, efficient charge extraction and higher electrical conductivity. Chandrasekhar et al.[131] prepared a PSC with nitrogen-doped graphene(NG)/ZnO nanorod composite ETL and obtained a PCE of 16.8%, compared with 12.9% for pristine ZnO nanorods. The enhanced PCE was attributed to the relatively high surface area and improved crystallinity of NG/ZnO composite when compared with pristine ZnO. Bi et al.[132] reported a device with N-doped graphene/fullerene derivative phenyl-$C_{61}$-butyric acid methyl ester (G-PCBM) as an electron extraction layer and obtained an initial PCE of 15.6%. The use of PCBM with G formed a good Ohmic contact of G-PCBM with a metal electrode, resulting in higher electrical conductivity and reduced hysteresis. They noted that the increase in the concentration of G was related to an increase in the grain size and crystallinity of the perovskite harvester.

Duan et al.[133] employed a B-doped graphene HTL in a PSC device and obtained a PCE of 13.6%. Their device demonstrated an improvement in hole extraction, which shielded the perovskite layer as the harvester, resulting in an improved FF and $V_{oc.}$[133] Selvakumar et al.[90] replaced the high-cost spiro-OMeTAD HTL with B-RGO, which resulted in PSCs with a relatively high PCE of 9.0%. In the presence of B, both $J_{sc}$ and $V_{oc}$ were improved, which resulted in an enhanced efficiency. A similar trend of enhanced efficiency was observed when B was doped onto graphene by Fang et al.[134] In this regard, doping B onto graphene (by replacing C with B) enhances the work function, conductivity and charge extraction; thus, improving the device performance. Kim et al.[135] synthesized a stable device from N-doped GO nanoribbons as HTLs, and obtained an enhanced PCE of 12.9%. The study obtained a low current hysteresis

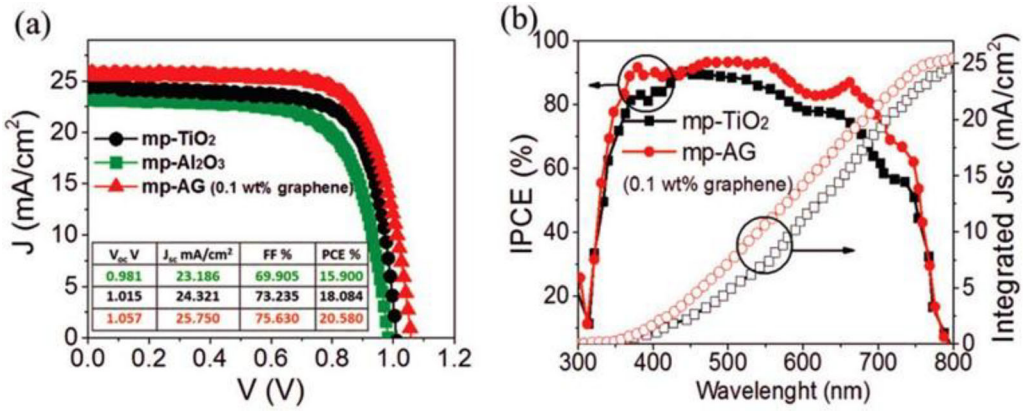


**Figure 15.** (a) J-V characteristics and (b) IPCE spectra of various materials preparing PSC devices. Adapted with permission.125 Copyright 2019, John Wiley and Sons.

and improved stability when GO was doped with N. Also, the introduction of N reduced the recombination rate, increased the grain size, enhanced the optical properties and improved the morphology features of graphene, resulting in enhanced device performance. On the other hand, the co-doping of N and S onto GQDs as NSGQDs has been explored by Chen et al.,[136] and they obtained a high PCE of 19.2%. The use of NSGQDs as an ETL promoted charge separation and reduced the recombination rate, while good stability and proper band alignment were observed between the HTL and perovskite harvester when NSGQDs HTLs were used.

### 7.3. Perovskite oxides

With low-cost, high PCE and long-term stability, PSCs are favorable for good ETLs and HTLs. In addition, PSCs have good resilience toward moisture, heat and light, and excellent electrical properties.[137] So far, $TiO_2$ has been the commonly used ETL in PSCs; however, its use is being limited by poor electron mobility.[138] Zhu et al.[138] prepared a mesoporous $BaSnO_3$ ETL with an enhanced PCE of 12.3% compared to 11.1% for $TiO_2$. Their findings noted that $BaSnO_3$ has a matching energy level with the light harvester, i.e., $CH_3NH_3PbI_3$, which promotes electron extraction and transportation. Also, they noted that $BaSnO_3$ has a high electron mobility, which results in efficient charge collection. Bera et al.[139] employed mesoporous $SrTiO_3$ with an average particle size of 230 nm, as an efficient ETL in hybrid PSCs. Increasing the loading thickness of $SrTiO_3$ from 200 to 350 nm provided good band alignment with the perovskite layer, resulting in relatively high $V_{oc}$, $J_{sc}$ and FF. This, in turn, resulted in PSCs with a PCE of 7.55%, which was slightly lower than 7.80% for mesoporous $TiO_2$.

Limited studies have reported the use of perovskite oxides as HTLs in PSCs. For example, Yang et al.[140] fabricated PSCs using ferroelectric $PbTiO_3$ as the HTL material. They noted an increase in $PbTiO_3$ particle sizes to more than 10 nm and HTL thickness from 1 to 10 nm when the $Pb(OAc)_2$ concentration was increased from 0.01 to 0.1 M. This gave rise to PSCs with a high PCE of 16.37%, which was attributed to the suppression of non-radiative recombination. However, HTLs prepared using perovskite oxides only still experience relatively high charge carrier recombination rates. Thus, integrating graphene with perovskite oxides would be a better choice to minimize charge carrier recombination.

### 7.4. Perovskite oxide/graphene nanocomposites

Few studies have reported perovskite oxide/graphene nanocomposites, particularly applied as interfacial layers in PSCs, even though these nanocomposites have great potential in this field. PSCs can easily suffer from the recombination of charge carriers and can be easily degraded by moisture, which in turn reduces the PCE and stability of devices. The combination of $\pi$-conjugated graphene materials and perovskite oxides containing Fe can narrow the energy bandgap to produce a redshift and collect solar radiation in a wider spectral range.[141] Wang et al.[142] prepared an effective ETL consisting of graphene/$SrTiO_3$ nanocomposites and obtained a PCE of 10.0%. They observed that the presence of the nanocomposites reduced the recombination rate and enhanced the absorption of light. Mamoudi et al.[124] also designed a highly stable device with $SrTiO_3/Al_2O_3$-graphene as an ETL. They observed a high PCE of up to 20.6%, as shown in

Figure 15. The use of $SrTiO_3$ contributed to a smaller band offset, which resulted in an excellent collection of photogenerated electrons from the perovskite layer. The use of graphene-based materials to form nanocomposites resulted in highly conductive ETLs, which had excellent electron mobility, charge extraction and balance of charge carriers. The graphene-based materials also enhanced the $J_{sc}$ and open-circuit voltage ($V_{oc}$) of the PSCs due to their faster electron accepting capability. Hence, incorporating graphene onto perovskite oxides can improve electron transport, and increase the electrical conductivity charge carrier mobility, thereby enhancing the PCE performance of PSCs. Therefore, perovskite oxide/graphene nanocomposites as HTLs of PSCs still need further research to be conducted in the future.

## 8 Conclusion and outlook

In conclusion, different graphene-based materials have been investigated as interfacial layers of PSCs. The PSCs can be used as a renewable energy system to harness sunlight and generate electricity without polluting the environment. The use of typical metal oxides, such as $TiO_2$ as ETLs, and organic HTLs, such as spiro-OMeTAD, can cause the device to degrade easily, and thus, lead to poor device performance. Interestingly, the use of graphene-based materials improves the performance of the device and offers long-term operational stability. Also, heteroatom-doped graphene produces n-type or p-type conductivity, altering the Fermi level and enhancing the optical properties of graphene, thereby allowing it to function as a substitute for the traditional metal oxide ETLs and organic HTLs. Any distortion, such as size and structure, on perovskite materials, can positively influence different properties, such as the electronic, optical, magnetic and dielectric properties. Moreover, the photogeneration of charge carriers can also be enhanced. When preparing nanocomposites, it is highly essential to consider the cost of materials and environmental safety. Perovskite oxides have been supported on graphene or doped graphene to form hydrophobic nanocomposites that are resistant to humidity penetration. Structures and sizes of perovskite oxides have played a considerable role in tuning the physical and chemical properties of the desired application. Synthetic protocols for preparing the nanocomposites can improve the homogeneity of the structures, reduce the synthesis time, and ensure good reproducibility. Therefore, perovskite oxide/graphene nanocomposites can function as good interfacial layers with high electrical conductivity, suitable for solar cell application. This review is envisaged to shed more light on the advancement of perovskite solar cell fabrications.

## Acknowledgments

The authors would like to thank Prof. Bice S. Martincigh and Mr. Nicholas Rono for their contributions and manuscript proofreading.

## Disclosure statement

The authors declare no conflict of interest.

## Funding

The authors sincerely thank the University of KwaZulu-Natal (UKZN); National Research Foundation (NRF) under Grant number 107740; Moses Kotane Institution, UKZN Nanotechnology Platform and Eskom Tertiary Education Support Programme (TESP) for their support and funding of this research.

## ORCID

Samantha Ndlovu http://orcid.org/0000-0001-7817-6119
Moses A. Ollengo http://orcid.org/0000-0002-8649-0578
Edigar Muchuweni http://orcid.org/0000-0002-7520-9154
Vincent O. Nyamori http://orcid.org/0000-0002-8995-4593

## References

1. Noh, J. H.; Im, S. H.; Heo, J. H.; Mandal, T. N.; Seok, S. I. Chemical Management for Colorful, Efficient, and Stable Inorganic-Organic Hybrid Nanostructured Solar Cells. *Nano Lett.* 2013, ***13***, 1764–1769. doi:10.1021/nl400349b
2. Correa Baena, J. P.; Steier, L.; Tress, W.; Saliba, M.; Neutzner, S.; Matsui, T.; Giordano, F.; Jacobsson, T. J.; Srimath Kandada, A. R.; Zakeeruddin, S. M.; et al. Highly Efficient Planar Perovskite Solar Cells through Band Alignment Engineering. *Energy Environ. Sci.* 2015, ***8***, 2928–2934., doi:10.1039/C5EE02608C
3. Wu, C.-G.; Chiang, C.-H.; Tseng, Z.-L.; Nazeeruddin, M. K.; Hagfeldt, A.; Grätzel, M. High Efficiency Stable Inverted Perovskite Solar Cells without Current Hysteresis. *Energy Environ. Sci.* 2015, ***8***, 2725–2733. doi:10.1039/C5EE00645G
4. Tan, H.; Jain, A.; Voznyy, O.; Lan, X.; García de Arquer, F. P.; Fan, J. Z.; Quintero-Bermudez, R.; Yuan, M.; Zhang, B.; Zhao, Y.; et al. Efficient and Stable Solution-Processed Planar Perovskite Solar Cells via Contact Passivation. *Science* 2017, ***355***, 722–726., doi:10.1126/science.aai9081
5. Saliba, M.; Matsui, T.; Domanski, K.; Seo, J.-Y.; Ummadisingu, A.; Zakeeruddin, S. M.; Correa-Baena, J.-P.; Tress, W. R.; Abate, A.; Hagfeldt, A.;

Grätzel, M. Incorporation of Rubidium Cations into Perovskite Solar Cells Improves Photovoltaic Performance. *Science* 2016, ***354***, 206–209. doi:10.1126/science.aah5557

6. Giordano, F.; Abate, A.; Correa Baena, J. P.; Saliba, M.; Matsui, T.; Im, S. H.; Zakeeruddin, S. M.; Nazeeruddin, M. K.; Hagfeldt, A.; Graetzel, M. Enhanced Electronic Properties in Mesoporous $TiO_2$ via Lithium Doping for High-Efficiency Perovskite Solar Cells. *Nat. Commun.* 2016, ***7***, 10379. doi:10.1038/ncomms10379
7. Chiang, C.-H.; Nazeeruddin, M. K.; Grätzel, M.; Wu, C.-G. The Synergistic Effect of $H_2O$ and DMF towards Stable and 20% Efficiency Inverted Perovskite Solar Cells. *Energy Environ. Sci.* 2017, ***10***, 808–817. doi:10.1039/C6EE03586H
8. Gu, P.-Y.; Wang, N.; Wang, C.; Zhou, Y.; Long, G.; Tian, M.; Chen, W.; Sun, X. W.; Kanatzidis, M. G.; Zhang, Q. Pushing up the Efficiency of Planar Perovskite Solar Cells to 18.2% with Organic Small Molecules as the Electron Transport Layer. *J. Mater. Chem. A.* 2017, ***5***, 7339–7344. doi:10.1039/C7TA01764B
9. Safie, N. E.; Azam, M. A.; Aziz, M. F.; Ismail, M. Recent Progress of Graphene-Based Materials for Efficient Charge Transfer and Device Performance Stability in Perovskite Solar Cells. *Int. J. Energy Res.* 2021, ***45***, 1347–1374. doi:10.1002/er.5876
10. Hailegnaw, B.; Paek, S.; Cho, K. T.; Lee, Y.; Ongül, F.; Nazeeruddin, M. K.; Scharber, M. C. Optoelectronic Properties of Layered Perovskite Solar Cells. *Sol. RRL* 2019, ***3***, 1900126. doi:10.1002/solr.201900126
11. Yan, K.; Wei, Z.; Li, J.; Chen, H.; Yi, Y.; Zheng, X.; Long, X.; Wang, Z.; Wang, J.; Xu, J.; Yang, S. High-Performance Graphene-Based Hole Conductor-Free Perovskite Solar Cells: Schottky Junction Enhanced Hole Extraction and Electron Blocking. *Small* 2015, ***11***, 2269–2274. doi:10.1002/smll.201403348
12. Yu, M.; Guo, Y.; Yuan, S.; Zhao, J.-S.; Qin, Y.; Ai, X.-C. The Influence of the Electron Transport Layer on Charge Dynamics and Trap-State Properties in Planar Perovskite Solar Cells. *RSC Adv.* 2020, ***10***, 12347–12353. doi:10.1039/D0RA00375A
13. Das, S.; Pandey, D.; Thomas, J.; Roy, T. The Role of Graphene and Other 2D Materials in Solar Photovoltaics. *Adv. Mater.* 2019, ***31***, 1802722. doi:10.1002/adma.201802722
14. Galal, A.; Hassan, H. K.; Atta, N. F.; Abdel-Mageed, A. M.; Jacob, T. Synthesis, Structural and Morphological Characterizations of Nano-Ru-Based Perovskites/RGO Composites. *Sci. Rep.* 2019, ***9***, 7948. doi:10.1038/s41598-019-43726-1
15. Sedeek, K.; Said, S. A.; Amer, T.; Makram, N.; Hantour, H. Band Gap Tuning in Nanocrystalline $SrTi_{0.9}Fe_{0.1}O_{2.968}$ Perovskite Type for Photocatalytic and Photovoltaic Applications. *Ceram. Int.* 2019, ***45***, 1202–1207. doi:10.1016/j.ceramint.2018.09.305
16. Fu, Y.; Zhu, J.; Hu, C.; Wu, X.; Wang, X. Covalently Coupled Hybrid of Graphitic Carbon Nitride with Reduced Graphene Oxide as a Superior Performance Lithium-Ion Battery Anode. *Nanoscale* 2014, ***6***, 12555–12564. doi:10.1039/c4nr03145h
17. Ambrosetti, A.; Silvestrelli, P. L. Anomalous Van Der Waals-Casimir Interactions on Graphene: A Concerted Effect of Temperature, Retardation, and Non-Locality. *J. Chem. Phys.* 2018, ***148***, 134709. doi:10.1063/1.5023170
18. Ayiania, M.; Hensley, A. J.; Groden, K.; Garcia-Perez, M.; McEwen, J.-S. Thermodynamic Stability of Nitrogen Functionalities and Defects in Graphene and Graphene Nanoribbons from First Principles. *Carbon* 2019, ***152***, 715–726. doi:10.1016/j.carbon.2019.06.019
19. Starowicz, Z.; Gawlińska, K.; Walter, J.; Socha, R. P.; Kulesza-Matlak, G.; Lipiński, M. Extended Investigation of Sol Aging Effect on $TiO_2$ Electron Transporting Layer and Performances of Perovskite Solar Cells. *Mater. Res. Bull.* 2018, ***99***, 136–143. doi:10.1016/j.materresbull.2017.10.035
20. Said, A. A.; Xie, J.; Zhang, Q. Recent Progress in Organic Electron Transport Materials in Inverted Perovskite Solar Cells. *Small* 2019, ***15***, 1900854. doi:10.1002/smll.201900854
21. Amollo, T. A.; Mola, G. T.; Nyamori, V. O. Organic Solar Cells: Materials and Prospects of Graphene for Active and Interfacial Layers. *Crit. Rev. Solid State Mater. Sci.* 2020, ***45***, 261–288. doi:10.1080/10408436.2019.1632791
22. Cao, J.; Yin, J.; Yuan, S.; Zhao, Y.; Li, J.; Zheng, N. Thiols as Interfacial Modifiers to Enhance the Performance and Stability of Perovskite Solar Cells. *Nanoscale* 2015, ***7***, 9443–9447. doi:10.1039/c5nr01820j
23. Hu, W.; Liu, T.; Yin, X.; Liu, H.; Zhao, X.; Luo, S.; Guo, Y.; Yao, Z.; Wang, J.; Wang, N.; et al. Hematite Electron-Transporting Layers for Environmentally Stable Planar Perovskite Solar Cells with Enhanced Energy Conversion and Lower Hysteresis. *J. Mater. Chem. A.* 2017, ***5***, 1434–1441., doi:10.1039/C6TA09174A
24. Wei, Z.; Chen, H.; Yan, K.; Zheng, X.; Yang, S. Hysteresis-Free Multi-Walled Carbon Nanotube-Based Perovskite Solar Cells with a High Fill Factor. *J. Mater. Chem. A.* 2015, ***3***, 24226–24231. doi:10.1039/C5TA07714A
25. Said, A. A.; Xie, J.; Wang, Y.; Wang, Z.; Zhou, Y.; Zhao, K.; Gao, W. B.; Michinobu, T.; Zhang, Q. Efficient Inverted Perovskite Solar Cells by Employing N-Type (D–A1–D–A2) Polymers as Electron Transporting Layer. *Small* 2019, ***15***, 1803339. doi:10.1002/smll.201803339
26. Yang, X.; Wang, H.; Cai, B.; Yu, Z.; Sun, L. Progress in Hole-Transporting Materials for Perovskite Solar Cells. *J. Energy Chem.* 2018, ***27***, 650–672. doi:10.1016/j.jechem.2017.12.017
27. Palma, A. L.; Cinà, L.; Pescetelli, S.; Agresti, A.; Raggio, M.; Paolesse, R.; Bonaccorso, F.; Carlo, A. D. Reduced Graphene Oxide as Efficient and Stable Hole Transporting Material in Mesoscopic Perovskite Solar Cells. *Nano Energy* 2016, ***22***, 349–360. doi:10.1016/j.nanoen.2016.02.027
28. Kim, H.-S.; Lee, C.-R.; Im, J.-H.; Lee, K.-B.; Moehl, T.; Marchioro, A.; Moon, S.-J.; Humphry-Baker, R.;

Yum, J.-H.; Moser, J. E.; et al. Lead Iodide Perovskite Sensitized All-Solid-State Submicron Thin Film Mesoscopic Solar Cell with Efficiency Exceeding 9%. *Sci. Rep.* 2012, ***2***, 591–597., doi:10.1038/srep00591

29. Burschka, J.; Pellet, N.; Moon, S.-J.; Humphry-Baker, R.; Gao, P.; Nazeeruddin, M. K.; Grätzel, M. Sequential Deposition as a Route to High-Performance Perovskite-Sensitized Solar Cells. *Nature* 2013, ***499***, 316–319. doi:10.1038/nature12340
30. Green, M. A.; Ho-Baillie, A.; Snaith, H. J. The Emergence of Perovskite Solar Cells. *Nat Photonics* 2014, ***8***, 134.
31. Nie, W.; Tsai, H.; Asadpour, R.; Blancon, J.-C.; Neukirch, A. J.; Gupta, G.; Crochet, J. J.; Chhowalla, M.; Tretiak, S.; Alam, M. A.; et al. Solar cells. High-Efficiency Solution-Processed Perovskite Solar Cells with Millimeter-Scale Grains . *Science* 2015, ***347***, 522–525., doi:10.1126/science.aaa0472
32. Chen, Q.; Zhou, H.; Hong, Z.; Luo, S.; Duan, H.-S.; Wang, H.-H.; Liu, Y.; Li, G.; Yang, Y. Planar Heterojunction Perovskite Solar Cells via Vapor-Assisted Solution Process. *J. Am. Chem. Soc.* 2014, ***136***, 622–625. doi:10.1021/ja411509g
33. Magomedov, A.; Paek, S.; Gratia, P.; Kasparavicius, E.; Daskeviciene, M.; Kamarauskas, E.; Gruodis, A.; Jankauskas, V.; Kantminiene, K.; Cho, K. T.; et al. Diphenylamine-Substituted Carbazole-Based Hole Transporting Materials for Perovskite Solar Cells: influence of Isomeric Serivatives. *Adv. Funct. Mater.* 2018, ***28***, 1704351., doi:10.1002/adfm.201704351
34. Zhao, D.; Sexton, M.; Park, H. Y.; Baure, G.; Nino, J. C.; So, F. High-Efficiency Solution-Processed Planar Perovskite Solar Cells with a Polymer Hole Transport Layer. *Adv. Energy Mater.* 2015, ***5***, 1401855. doi:10.1002/aenm.201401855
35. Habisreutinger, S. N.; Leijtens, T.; Eperon, G. E.; Stranks, S. D.; Nicholas, R. J.; Snaith, H. J. Carbon Nanotube/Polymer Composites as a Highly Stable Hole Collection Layer in Perovskite Solar Cells. *Nano Lett.* 2014, ***14***, 5561–5568. doi:10.1021/nl501982b
36. Castro-Hermosa, S.; Yadav, S.; Vesce, L.; Guidobaldi, A.; Reale, A.; Carlo, A. D.; Brown, T. Stability Issues Pertaining Large Area Perovskite and Dye-Sensitized Solar Cells and Modules. *J. Phys. D: Appl. Phys.* 2017, ***50***, 033001. doi:10.1088/1361-6463/50/3/033001
37. Niu, G.; Guo, X.; Wang, L. Review of Recent Progress in Chemical Stability of Perovskite Solar Cells. *J. Mater. Chem. A.* 2015, ***3***, 8970–8980. doi:10.1039/C4TA04994B
38. Qin, X.; Zhao, Z.; Wang, Y.; Wu, J.; Jiang, Q.; You, J. Recent Progress in Stability of Perovskite Solar Cells. *J. Semicond.* 2017, ***38***, 011002–011012. doi:10.1088/1674-4926/38/1/011002
39. Meng, L.; You, J.; Guo, T.-F.; Yang, Y. Recent Advances in the Inverted Planar Structure of Perovskite Solar Cells. *Acc. Chem. Res.* 2016, ***49***, 155–165. doi:10.1021/acs.accounts.5b00404
40. You, J.; Meng, L.; Song, T.-B.; Guo, T.-F.; Yang, Y. M.; Chang, W.-H.; Hong, Z.; Chen, H.; Zhou, H.; Chen, Q.; et al. Improved Air Stability of Perovskite Solar Cells via Solution-Processed Metal Oxide Transport Layers. *Nat. Nanotechnol.* 2016, ***11***, 75–81., doi:10.1038/nnano.2015.230
41. Domanski, K.; Correa-Baena, J.-P.; Mine, N.; Nazeeruddin, M. K.; Abate, A.; Saliba, M.; Tress, W.; Hagfeldt, A.; GräTzel, M. Not All That Glitters is Gold: metal-Migration-Induced Degradation in Perovskite Solar Cells. *ACS Nano.* 2016, ***10***, 6306–6314. doi:10.1021/acsnano.6b02613
42. Shin, S. S.; Yeom, E. J.; Yang, W. S.; Hur, S.; Kim, M. G.; Im, J.; Seo, J.; Noh, J. H.; Seok, S. I. Colloidally Prepared La-Doped $BaSnO_3$ Electrodes for Efficient, Photostable Perovskite Solar Cells. *Science* 2017, ***356***, 167–171. doi:10.1126/science.aam6620
43. Lim, E. L.; Yap, C. C.; Jumali, M. H. H.; Teridi, M. A. M.; Teh, C. H. A Mini Review: Can Graphene Be a Novel Material for Perovskite Solar Cell Applications? *Nanomicro. Lett.* 2018, ***10***, 27.
44. Wang, J.; Dong, J.; Lu, F.; Sun, C.; Zhang, Q.; Wang, N. Two-Dimensional Lead-Free Halide Perovskite Materials and Devices. *J. Mater. Chem. A.* 2019, ***7***, 23563–23576. doi:10.1039/C9TA06455A
45. Chung, I.; Lee, B.; He, J.; Chang, R. P. H.; Kanatzidis, M. G. All-Solid-State Dye-Sensitized Solar Cells with High Efficiency. *Nature* 2012, ***485***, 486–489. doi:10.1038/nature11067
46. Im, J.-H.; Lee, C.-R.; Lee, J.-W.; Park, S.-W.; Park, N.-G. 6.5% Efficient Perovskite Quantum-Dot-Sensitized Solar Cell. *Nanoscale* 2011, ***3***, 4088–4093. doi:10.1039/c1nr10867k
47. Lee, M. M.; Teuscher, J.; Miyasaka, T.; Murakami, T. N.; Snaith, H. J. Efficient Hybrid Solar Cells Based on Meso-Superstructured Organometal Halide Perovskites. *Science* 2012, ***338***, 643–647. doi:10.1126/science.1228604
48. Xiao, Z.; Zhou, Y.; Hosono, H.; Kamiya, T.; Padture, N. P. Bandgap Optimization of Perovskite Semiconductors for Photovoltaic Applications. *Chemistry* 2018, ***24***, 2305–2316. doi:10.1002/chem.201705031
49. Akhtar, S.; Alay-e-Abbas, S. M.; Abbas, S. M. G.; Arshad, M. I.; Batool, J.; Amin, N. First-Principles Evaluation of Electronic and Optical Properties of (Mo, C) Codoped $BaHfO_3$ for Applications in Photocatalysis. *J. Appl. Phys.* 2018, ***123***, 161569. doi:10.1063/1.5010969
50. Wang, N.; Liu, W.; Zhang, Q. Perovskite-Based Nanocrystals: Synthesis and Applications beyond Solar Cells. *Small Methods* 2018, ***2***, 1700380. doi:10.1002/smtd.201700380
51. Wang, W.; Lin, B.; Zhang, H.; Sun, Y.; Zhang, X.; Yang, H. Synthesis, Morphology and Electrochemical Performances of Perovskite-Type Oxide $La_xSr_{1-x}FeO_3$ Nanofibers Prepared by Electrospinning. *J. Phys. Chem. Solids* 2019, ***124***, 144–150. doi:10.1016/j.jpcs.2018.09.011
52. Njoku, C. B.; Omondi, B.; Ndungu, P. Effect of Surfactants on the Physico-Chemical Characteristics of $IrO/Ce_{0.8}Sm_{0.2}O_{2-\delta}$ Nanocomposite for SOFC Application. *ECS Trans.* 2017, ***78***, 783–793. doi:10.1149/07801.0783ecst

53. Jia, L.; Li, J.; Fang, W. Effect of $H_2/CO_2$ Mixture Gas Treatment Temperature on the Activity of $LaNiO_3$ Catalyst for Hydrogen Production from Formaldehyde Aqueous Solution under Visible Light. *J. Alloys Compd.* 2010, ***489***, L13–L16. doi:10.1016/j.jallcom.2009.09.104
54. Wei, Z.-X.; Xu, Y.-Q.; Liu, H.-Y.; Hu, C.-W. Preparation and Catalytic Activities of $LaFeO_3$ and $Fe_2O_3$ for HMX Thermal Decomposition. *J. Hazard. Mater.* 2009, ***165***, 1056–1061. doi:10.1016/j.jhazmat.2008.10.086
55. Mao, C.; Wu, X.; Zhu, J.-J. Large Scale Preparation of beta-AgVO3 Nanowires Using a Novel Sonochemical Route. *J. Nanosci. Nanotechnol.* 2008, ***8***, 3203–3207. doi:10.1166/jnn.2008.102
56. Aman, D.; Zaki, T.; Mikhail, S.; Selim, S. Synthesis of a Perovskite $LaNiO_3$ Nanocatalyst at a Low Temperature Using Single Reverse Microemulsion. *Catal. Today* 2011, ***164***, 209–213. doi:10.1016/j.cattod.2010.11.034
57. Fan, H.-T.; Xu, X.-J.; Ma, X.-K.; Zhang, T. Preparation of $LaFeO_3$ Nanofibers by Electrospinning for Gas Sensors with Fast Response and Recovery. *Nanotechnology* 2011, ***22***, 115502. doi:10.1088/0957-4484/22/11/115502
58. Tien, N. A.; Almjasheva, O.; Mittova, I. Y.; Stognei, O.; Soldatenko, S. Synthesis and Magnetic Properties of $YFeO_3$ Nanocrystals. *Inorg. Mater.* 2009, ***45***, 1304–1308. doi:10.1134/S0020168509110211
59. Chen, Z.; Fan, T.; Zhang, Q.; He, J.; Fan, H.; Sun, Y.; Yi, X.; Li, J. Interface Engineering: Surface Hydrophilic Regulation of $LaFeO_3$ towards Enhanced Visible Light Photocatalytic Hydrogen Evolution. *J. Colloid Interface Sci.* 2019, ***536***, 105–111. doi:10.1016/j.jcis.2018.10.030
60. Fu, Y.; Wang, X. Magnetically Separable $ZnFe_2O_4$–Graphene Catalyst and Its High Photocatalytic Performance under Visible Light Irradiation. *Ind. Eng. Chem. Res.* 2011, ***50***, 7210–7218. doi:10.1021/ie200162a
61. Guo, R.; Fang, L.; Dong, W.; Zheng, F.; Shen, M. Enhanced Photocatalytic Activity and Ferromagnetism in Gd Doped $BiFeO_3$ Nanoparticles. *J. Phys. Chem. C.* 2010, ***114***, 21390–21396. doi:10.1021/jp104660a
62. Hu, J.; Wang, L.; Shi, L.; Huang, H. Oxygen Reduction Reaction Activity of $LaMn_{1-x}Co_xO_3$-Graphene Nanocomposite for Zinc-Air Battery. *Electrochim Acta* 2015, ***161***, 115–123. doi:10.1016/j.electacta.2015.02.048
63. Li, D.; Bretschneider, S. A.; Bergmann, V. W.; Hermes, I. M.; Mars, J.; Klasen, A.; Lu, H.; Tremel, W.; Mezger, M.; Butt, H.-J.; et al. Humidity-Induced Grain Boundaries in $MAPbI_3$ Perovskite Films. *J. Phys. Chem. C.* 2016, ***120***, 6363–6368., doi:10.1021/acs.jpcc.6b00335
64. Nouri, E.; Wang, Y.-L.; Chen, Q.; Xu, J.-J.; Paterakis, G.; Dracopoulos, V.; Xu, Z.-X.; Tasis, D.; Mohammadi, M. R.; Lianos, P. Introduction of Graphene Oxide as Buffer Layer in Perovskite Solar Cells and the Promotion of Soluble n-Butyl-Substituted Copper Phthalocyanine as Efficient Hole Transporting Material. *Electrochim Acta* 2017, ***233***, 36–43. doi:10.1016/j.electacta.2017.03.027
65. Wang, Z.; Wu, S.; Zhang, J.; Chen, P.; Yang, G.; Zhou, X.; Zhang, Q.; Yan, Q.; Zhang, H. Comparative Studies on Single-Layer Reduced Graphene Oxide Films Obtained by Electrochemical Reduction and Hydrazine Vapor Reduction. *Nanoscale Res. Lett.* 2012, ***7***, 161–167. doi:10.1186/1556-276X-7-161
66. Yan, X.; Cui, X.; Li, B.; Li, L-s. Large, Solution-Processable Graphene Quantum Dots as Light Absorbers for Photovoltaics. *Nano Lett.* 2010, ***10***, 1869–1873. doi:10.1021/nl101060h
67. Bai, J.; Zhong, X.; Jiang, S.; Huang, Y.; Duan, X. Graphene Nanomesh. *Nat. Nanotechnol.* 2010, ***5***, 190–194. doi:10.1038/nnano.2010.8
68. Rafiee, M. A.; Lu, W.; Thomas, A. V.; Zandiatashbar, A.; Rafiee, J.; Tour, J. M.; Koratkar, N. A. Graphene Nanoribbon Composites. *ACS Nano.* 2010, ***4***, 7415–7420. doi:10.1021/nn102529n
69. Liu, T.; Chen, K.; Hu, Q.; Zhu, R.; Gong, Q. Inverted Perovskite Solar Cells: Progresses and Perspectives. *Adv. Energy Mater.* 2016, ***6***, 1600457. doi:10.1002/aenm.201600457
70. Acik, M.; Darling, S. B. Graphene in Perovskite Solar Cells: device Design, Characterization and Implementation. *J. Mater. Chem. A.* 2016, ***4***, 6185–6235. doi:10.1039/C5TA09911K
71. Hass, J.; Heer, W. D.; Conrad, E. The Growth and Morphology of Epitaxial Multilayer Graphene. *J. Phys: Condens. Matter.* 2008, ***20***, 323202. doi:10.1088/0953-8984/20/32/323202
72. Lim, S. P.; Pandikumar, A.; Huang, N. M.; Lim, H. N. Reduced Graphene Oxide–Titania Nanocomposite-Modified Photoanode for Efficient Dye-Sensitized Solar Cells. *Int. J. Energy Res.* 2015, ***39***, 812–824. doi:10.1002/er.3307
73. Novoselov, K. S.; Geim, A. K.; Morozov, S. V.; Jiang, D.; Zhang, Y.; Dubonos, S. V.; Grigorieva, I. V.; Firsov, A. A. Electric Field Effect in Atomically Thin Carbon Films. *Science* 2004, ***306***, 666–669. doi:10.1126/science.1102896
74. Sung, H.; Ahn, N.; Jang, M. S.; Lee, J. K.; Yoon, H.; Park, N. G.; Choi, M. Transparent Conductive Oxide-Free Graphene-Based Perovskite Solar Cells with over 17% Efficiency. *Adv. Energy Mater.* 2016, ***6***, 1501873. doi:10.1002/aenm.201501873
75. Singh, E.; Nalwa, H. S. Graphene-Based Bulk-Heterojunction Solar Cells: A Review. *J. Nanosci. Nanotechnol.* 2015, ***15***, 6237–6278. doi:10.1166/jnn.2015.11654
76. Georgakilas, V.; Otyepka, M.; Bourlinos, A. B.; Chandra, V.; Kim, N.; Kemp, K. C.; Hobza, P.; Zboril, R.; Kim, K. S. Functionalization of Graphene: Covalent and Non-Covalent Approaches, Derivatives and Applications. *Chem. Rev.* 2012, ***112***, 6156–6214. doi:10.1021/cr3000412
77. Bouclé, J.; Herlin-Boime, N. The Benefits of Graphene for Hybrid Perovskite Solar Cells. *Synth. Met.* 2016, ***222***, 3–16. doi:10.1016/j.synthmet.2016.03.030

78. Allen, M. J.; Tung, V. C.; Kaner, R. B. Honeycomb Carbon: A Review of Graphene. *Chem. Rev.* 2010, ***110***, 132–145. doi:10.1021/cr900070d
79. Shin, S. H.; Shin, D. H.; Choi, S.-H. Enhancement of Stability of Inverted Flexible Perovskite Solar Cells by Employing Graphene-Quantum-Dots Hole Transport Layer and Graphene Transparent Electrode Codoped with Gold Nanoparticles and Bis(Trifluoromethanesulfonyl)Amide. *ACS Sustain. Chem. Eng.* 2019, ***7***, 13178–13185. doi:10.1021/acssuschemeng.9b02336
80. Zhao, S.; Lavie, J.; Rondin, L.; Orcin-Chaix, L.; Diederichs, C.; Roussignol, P.; Chassagneux, Y.; Voisin, C.; Müllen, K.; Narita, A.; et al. Single Photon Emission from Graphene Quantum Dots at Room Temperature. *Nat. Commun.* 2018, ***9***, 3470 doi:10.1038/s41467-018-05888-w
81. Yan, Y.; Gong, J.; Chen, J.; Zeng, Z.; Huang, W.; Pu, K.; Liu, J.; Chen, P. Recent Advances on Graphene Quantum Dots: From Chemistry and Physics to Applications. *Adv. Mater.* 2019, ***31***, 1808283. doi:10.1002/adma.201808283
82. Pang, S.; Zhang, C.; Zhang, H.; Dong, H.; Chen, D.; Zhu, W.; Xi, H.; Chang, J.; Lin, Z.; Zhang, J.; Hao, Y. Boosting Performance of Perovskite Solar Cells with Graphene Quantum Dots Decorated $SnO_2$ Electron Transport Layers. *Appl. Surf. Sci.* 2020, ***507***, 145099. doi:10.1016/j.apsusc.2019.145099
83. Tiwari, S. K.; Kumar, V.; Huczko, A.; Oraon, R.; Adhikari, A. D.; Nayak, G. Magical Allotropes of Carbon: prospects and Applications. *Crit. Rev. Solid State Mater. Sci.* 2016, ***41***, 257–317. doi:10.1080/10408436.2015.1127206
84. Zhao, Y.; Hu, C.; Song, L.; Wang, L.; Shi, G.; Dai, L.; Qu, L. Functional Graphene Nanomesh Foam. *Energy Environ. Sci.* 2014, ***7***, 1913–1918. doi:10.1039/c4ee00106k
85. Kim, H.; Lim, K.-G.; Lee, T.-W. Planar Heterojunction Organometal Halide Perovskite Solar Cells: roles of Interfacial Layers. *Energy Environ. Sci.* 2016, ***9***, 12–30. doi:10.1039/C5EE02194D
86. Wang, X.; Sun, G.; Routh, P.; Kim, D.-H.; Huang, W.; Chen, P. Heteroatom-Doped Graphene Materials: Syntheses, Properties and Applications . *Chem. Soc. Rev.* 2014, ***43***, 7067–7098. doi:10.1039/c4cs00141a
87. Li, X.; Fan, L.; Li, Z.; Wang, K.; Zhong, M.; Wei, J.; Wu, D.; Zhu, H. Boron Doping of Graphene for Graphene–Silicon p–n Junction Solar Cells. *Adv. Energy Mater.* 2012, ***2***, 425–429. doi:10.1002/aenm.201100671
88. Faccio, R.; Fernández-Werner, L.; Pardo, H.; Goyenola, C.; Ventura, O. N.; Mombrú, Á. W. Electronic and Structural Distortions in Graphene Induced by Carbon Vacancies and Boron Doping. *J. Phys. Chem. C.* 2010, ***114***, 18961–18971. doi:10.1021/jp106764h
89. Rani, P.; Jindal, V. Designing Band Gap of Graphene by B and N Dopant Atoms. *RSC Adv.* 2013, ***3***, 802–812. doi:10.1039/C2RA22664B
90. Selvakumar, D.; Murugadoss, G.; Alsalme, A.; Alkathiri, A. M.; Jayavel, R. Heteroatom Doped Reduced Graphene Oxide Paper for Large Area Perovskite Solar Cells. *Sol. Energy* 2018, ***163***, 564–569. doi:10.1016/j.solener.2018.01.084
91. Zhang, C.; Hao, R.; Liao, H.; Hou, Y. Synthesis of Amino-Functionalized Graphene as Metal-Free Catalyst and Exploration of the Roles of Various Nitrogen States in Oxygen Reduction Reaction. *Nano Energy* 2013, ***2***, 88–97. doi:10.1016/j.nanoen.2012.07.021
92. Wang, H.; Maiyalagan, T.; Wang, X. Review on Recent Progress in Nitrogen-Doped Graphene: synthesis, Characterization, and Its Potential Applications. *ACS Catal.* 2012, ***2***, 781–794. doi:10.1021/cs200652y
93. Panchakarla, L.; Subrahmanyam, K.; Saha, S.; Govindaraj, A.; Krishnamurthy, H.; Waghmare, U.; Rao, C. Synthesis, Structure, and Properties of Boron-and Nitrogen-Doped Graphene. *Adv. Mater.* 2009, ***21***, NA–4730. doi:10.1002/adma.200901285
94. Hadadian, M.; Correa-Baena, J.-P.; Goharshadi, E. K.; Ummadisingu, A.; Seo, J.-Y.; Luo, J.; Gholipour, S.; Zakeeruddin, S. M.; Saliba, M.; Abate, A.; et al. Enhancing Efficiency of Perovskite Solar Cells via N-doped Graphene: Crystal Modification and Surface Passivation. *Adv. Mater.* 2016, ***28***, 8681–8686., doi:10.1002/adma.201602785
95. Zhu, Y.; Jia, S.; Zheng, J.; Lin, Y.; Wu, Y.; Wang, J. Facile Synthesis of Nitrogen-Doped Graphene Frameworks for Enhanced Performance of Hole Transport Material-Free Perovskite Solar Cells. *J. Mater. Chem. C.* 2018, ***6***, 3097–3103. doi:10.1039/C8TC00086G
96. Chen, M.; Zha, R.-H.; Yuan, Z.-Y.; Jing, Q.-S.; Huang, Z.-Y.; Yang, X.-K.; Yang, S.-M.; Zhao, X.-H.; Xu, D.-L.; Zou, G.-D. Boron and Phosphorus co-Doped Carbon Counter Electrode for Efficient Hole-Conductor-Free Perovskite Solar Cell. *Chem. Eng. J.* 2017, ***313***, 791–800. doi:10.1016/j.cej.2016.12.050
97. Kumar, P. V.; Bernardi, M.; Grossman, J. C. The Impact of Functionalization on the Stability, Work Function, and Photoluminescence of Reduced Graphene Oxide. *ACS Nano.* 2013, ***7***, 1638–1645. doi:10.1021/nn305507p
98. Luo, Q.; Hao, F.; Wang, S.; Shen, H.; Zhao, L.; Li, J.; Grätzel, M.; Lin, H. Highly Efficient Metal-Free Sulfur-Doped and Nitrogen and Sulfur Dual-Doped Reduced Graphene Oxide Counter Electrodes for Dye-Sensitized Solar Cells. *J. Phys. Chem. C.* 2014, ***118***, 17010–17018. doi:10.1021/jp5004424
99. Poh, H. L.; Simek, P.; Sofer, Z.; Pumera, M. Sulfur-Doped Graphene via Thermal Exfoliation of Graphite Oxide in $H_2S$, $SO_2$, or $CS_2$ Gas. *ACS Nano.* 2013, ***7***, 5262–5272. doi:10.1021/nn401296b
100. Chen, W.; Xiao, P.; Chen, H.; Zhang, H.; Zhang, Q.; Chen, Y. Polymeric Graphene Bulk Materials with a 3D Cross-Linked Monolithic Graphene Network. *Adv. Mater.* 2019, ***31***, 1802403. doi:10.1002/adma.201802403
101. Lu, J.; Zhu, J.; Wang, Z.; Cao, J.; Zhou, X. Rapid Synthesis and Thermal Catalytic Performance of N-Doped ZnO/Ag Nanocomposites. *Ceram. Int.* 2014, ***40***, 1489–1494. doi:10.1016/j.ceramint.2013.07.033

102. Zhu, Y.; Zhou, W.; Shao, Z. Perovskite/Carbon Composites: applications in Oxygen Electrocatalysis. *Small* 2017, ***13***, 1603793. doi:10.1002/smll.201603793
103. Dai, L.; Liu, M.; Song, Y.; Liu, J.; Wang, F. $Mn_3O_4$-Decorated $Co_3O_4$ Nanoparticles Supported on Graphene Oxide: dual Electrocatalyst System for Oxygen Reduction Reaction in Alkaline Medium. *Nano Energy* 2016, ***27***, 185–195. doi:10.1016/j.nanoen.2016.07.007
104. Tan, G. Q.; Zheng, Y. Q.; Miao, H. Y.; Xia, A.; Ren, H. J. Controllable Microwave Hydrothermal Synthesis of Bismuth Ferrites and Photocatalytic Characterization. *J. Am. Ceram. Soc.* 2012, ***95***, 280–289. doi:10.1111/j.1551-2916.2011.04775.x
105. Vijayan, B. K.; Dimitrijevic, N. M.; Wu, J.; Gray, K. A. The Effects of Pt Doping on the Structure and Visible Light Photoactivity of Titania Nanotubes. *J. Phys. Chem. C.* 2010, ***114***, 21262–21269. doi:10.1021/jp108659a
106. Sun, A.; Chen, H.; Song, C.; Jiang, F.; Wang, X.; Fu, Y. Magnetic $Bi_{25}FeO_{40}$-Graphene Catalyst and Its High Visible-Light Photocatalytic Performance. *RSC Adv.* 2013, ***3***, 4332–4340. doi:10.1039/c3ra22626c
107. Nayak, S.; Soam, A.; Nanda, J.; Mahender, C.; Singh, M.; Mohapatra, D.; Kumar, R. Sol–Gel Synthesized $BiFeO_3$–Graphene Nanocomposite as Efficient Electrode for Supercapacitor Application. *J. Mater. Sci: Mater. Electron.* 2018, ***29***, 9361–9368. doi:10.1007/s10854-018-8967-6
108. Teja, A. S.; Koh, P.-Y. Synthesis, Properties, and Applications of Magnetic Iron Oxide Nanoparticles. *Prog. Cryst. Growth Charact. Mater.* 2009, ***55***, 22–45. doi:10.1016/j.pcrysgrow.2008.08.003
109. Hu, Z.-T.; Liu, J.; Yan, X.; Oh, W.-D.; Lim, T.-T. Low-Temperature Synthesis of Graphene/$Bi_2Fe_4O_9$ Composite for Synergistic Adsorption-Photocatalytic Degradation of Hydrophobic Pollutant under Solar Irradiation. *Chem. Eng. J.* 2015, ***262***, 1022–1032. doi:10.1016/j.cej.2014.10.037
110. Sagayaraj, R.; Aravazhi, S.; Chandrasekaran, G. Tuning of Ferrites ($Co_xFe_{3-x}O_4$) Nanoparticles by co-Precipitation Technique. *Appl. Sci.* 2019, ***1***, 271.
111. Sanchez-Martinez, A.; Ortiz-Beas, J.; Huerta-Flores, A.; López-Mena, E. R.; Pérez-Álvarez, J.; Ceballos-Sanchez, O. ZnSe Nanoparticles Prepared by Coprecipitation Method for Photocatalytic Applications. *Mater. Lett.* 2021, ***282***, 128702. doi:10.1016/j.matlet.2020.128702
112. Cao, Y.; Zhang, L.; Tao, D.; Huo, D.; Su, K. Facile Synthesis of $CoSnO_3$/Graphene Nanohybrid with Superior Lithium Storage Capability. *Electrochim Acta* 2014, ***132***, 483–489. doi:10.1016/j.electacta.2014.03.048
113. Li, T.; Shen, J.; Li, N.; Ye, M. Hydrothermal Preparation, Characterization and Enhanced Properties of Reduced graphene-$BiFeO_3$ Nanocomposite. *Mater. Lett.* 2013, ***91***, 42–44. doi:10.1016/j.matlet.2012.09.045
114. Lu, D.; Zhang, Y.; Lin, S.; Wang, L.; Wang, C. Synthesis of Magnetic $ZnFe_2O_4$/Graphene Composite and Its Application in Photocatalytic Degradation of Dyes. *J. Alloys Compd.* 2013, ***579***, 336–342. doi:10.1016/j.jallcom.2013.06.098
115. Sethi, M.; Bhat, D. K. Facile Solvothermal Synthesis and High Supercapacitor Performance of $NiCo_2O_4$ Nanorods. *J. Alloys Compd.* 2019, ***781***, 1013–1020. doi:10.1016/j.jallcom.2018.12.143
116. Li, N.; Zheng, M.; Chang, X.; Ji, G.; Lu, H.; Xue, L.; Pan, L.; Cao, J. Preparation of Magnetic $CoFe_2O_4$-Functionalized Graphene Sheets via a Facile Hydrothermal Method and Their Adsorption Properties. *J. Solid State Chem.* 2011, ***184***, 953–958. doi:10.1016/j.jssc.2011.01.014
117. Wang, W.; Guo, S.; Zhang, D.; Yang, Z. One-Pot Hydrothermal Synthesis of Reduced Graphene Oxide/Zinc Ferrite Nanohybrids and Its Catalytic Activity on the Thermal Decomposition of Ammonium Perchlorate. *J. Saudi Chem. Soc.* 2019, ***23***, 133–140. doi:10.1016/j.jscs.2018.05.001
118. Hummers, W. S. Jr.; Offeman, R. E. Preparation of Graphitic Oxide. *J. Am. Chem. Soc.* 1958, ***80***, 1339–1339. doi:10.1021/ja01539a017
119. Singh, E.; Nalwa, H. S. Stability of Graphene-Based Heterojunction Solar Cells. *RSC Adv.* 2015, ***5***, 73575–73600. doi:10.1039/C5RA11771B
120. Milić, J. V.; Arora, N.; Dar, M. I.; Zakeeruddin, S. M.; Grätzel, M. Reduced Graphene Oxide as a Stabilizing Agent in Perovskite Solar Cells. *Adv. Mater. Interfaces* 2018, ***5***, 1800416. doi:10.1002/admi.201800416
121. Agresti, A.; Pescetelli, S.; Cinà, L.; Konios, D.; Kakavelakis, G.; Kymakis, E.; Carlo, A. D. Efficiency and Stability Enhancement in Perovskite Solar Cells by Inserting Lithium-Neutralized Graphene Oxide as Electron Transporting Layer. *Adv. Funct. Mater.* 2016, ***26***, 2686–2694. doi:10.1002/adfm.201504949
122. Nouri, E.; Mohammadi, M. R.; Lianos, P. Improving the Stability of Inverted Perovskite Solar Cells under Ambient Conditions with Graphene-Based Inorganic Charge Transporting Layers. *Carbon* 2018, ***126***, 208–214. doi:10.1016/j.carbon.2017.10.015
123. Şahin, Ç.; Diker, H.; Sygkridou, D.; Varlikli, C.; Stathatos, E. Enhancing the Efficiency of Mixed Halide Mesoporous Perovskite Solar Cells by Introducing Amine Modified Graphene Oxide Buffer Layer. *Renew. Energy* 2020, ***146***, 1659–1666. doi:10.1016/j.renene.2019.07.162
124. Mahmoudi, T.; Wang, Y.; Hahn, Y. B. $SrTiO_3$/$Al_2O_3$-Graphene Electron Transport Layer for Highly Stable and Efficient Composites-Based Perovskite Solar Cells with 20.6% Efficiency. *Adv. Energy Mater.* 2020, ***10***, 1903369. doi:10.1002/aenm.201903369
125. Wang, J. T.-W.; Ball, J. M.; Barea, E. M.; Abate, A.; Alexander-Webber, J. A.; Huang, J.; Saliba, M.; Mora-Sero, I.; Bisquert, J.; Snaith, H. J.; Nicholas, R. J. Low-Temperature Processed Electron Collection Layers of Graphene/$TiO_2$ Nanocomposites in Thin Film Perovskite Solar Cells. *Nano Lett.* 2014, ***14***, 724–730. doi:10.1021/nl403997a
126. Shen, D.; Zhang, W.; Xie, F.; Li, Y.; Abate, A.; Wei, M. Graphene Quantum Dots Decorated $TiO_2$ Mesoporous Film as an Efficient Electron Transport

Layer for High-Performance Perovskite Solar Cells. *J. Power Sources* 2018, ***402***, 320–326. doi:10.1016/j.jpowsour.2018.09.056

127. Yang, Z.; Xie, J.; Arivazhagan, V.; Xiao, K.; Qiang, Y.; Huang, K.; Hu, M.; Cui, C.; Yu, X.; Yang, D. Efficient and Highly Light Stable Planar Perovskite Solar Cells with Graphene Quantum Dots Doped PCBM Electron Transport Layer. *Nano Energy* 2017, ***40***, 345–351. doi:10.1016/j.nanoen.2017.08.008
128. Redondo-Obispo, C.; Ripolles, T.; Cortijo-Campos, S.; Álvarez, A.; Climent-Pascual, E.; de Andrés, A.; Coya, C. Enhanced Stability and Efficiency in Inverted Perovskite Solar Cells through Graphene Doping of PEDOT: PSS Hole Transport Layer. *Mater. Des.* 2020, ***191***, 108587. doi:10.1016/j.matdes.2020.108587
129. Yeo, J.-S.; Kang, R.; Lee, S.; Jeon, Y.-J.; Myoung, N.; Lee, C.-L.; Kim, D.-Y.; Yun, J.-M.; Seo, Y.-H.; Kim, S.-S.; Na, S.-I. Highly Efficient and Stable Planar Perovskite Solar Cells with Reduced Graphene Oxide Nanosheets as Electrode Interlayer. *Nano Energy* 2015, ***12***, 96–104. doi:10.1016/j.nanoen.2014.12.022
130. Hong, J. A.; Jung, E. D.; Yu, J. C.; Kim, D. W.; Nam, Y. S.; Oh, I.; Lee, E.; Yoo, J.-W.; Cho, S.; Song, M. H. Improved Efficiency of Perovskite Solar Cells Using a Nitrogen-Doped Graphene-Oxide-Treated Tin Oxide Layer. *ACS Appl. Mater. Interfaces* 2020, ***12***, 2417–2423. doi:10.1021/acsami.9b17705
131. Chandrasekhar, P.; Dubey, A.; Qiao, Q. High Efficiency Perovskite Solar Cells Using Nitrogen-Doped Graphene/ZnO Nanorod Composite as an Electron Transport Layer. *Sol. Energy* 2020, ***197***, 78–83. doi:10.1016/j.solener.2019.12.062
132. Bi, E.; Chen, H.; Xie, F.; Wu, Y.; Chen, W.; Su, Y.; Islam, A.; Grätzel, M.; Yang, X.; Han, L. Diffusion Engineering of Ions and Charge Carriers for Stable Efficient Perovskite Solar Cells. *Nat. Commun.* 2017, ***8***, 15330–15337. doi:10.1038/ncomms15330
133. Duan, M.; Tian, C.; Hu, Y.; Mei, A.; Rong, Y.; Xiong, Y.; Xu, M.; Sheng, Y.; Jiang, P.; Hou, X.; et al. Boron-Doped Graphite for High Work Function Carbon Electrode in Printable Hole-Conductor-Free Mesoscopic Perovskite Solar Cells. *ACS Appl. Mater. Interfaces* 2017, ***9***, 31721–31727., doi:10.1021/acsami.7b05689
134. Fang, H.; Yu, C.; Ma, T.; Qiu, J. Boron-Doped Graphene as a High-Efficiency Counter Electrode for Dye-Sensitized Solar Cells. *Chem. Commun.* 2014, ***50***, 3328–3330. doi:10.1039/c3cc48258h
135. Kim, J.; Mat Teridi, M. A.; Mohd Yusoff, A. R. b.; Jang, J. Stable and Null Current Hysteresis Perovskite Solar Cells Based Nitrogen Doped Graphene Oxide Nanoribbons Hole Transport Layer. *Sci. Rep.* 2016, ***6***, 27773. doi:10.1038/srep27773
136. Chen, H.; Luo, Q.; Liu, T.; Tai, M.; Lin, J.; Murugadoss, V.; Lin, H.; Wang, J.; Guo, Z.; Wang, N. Boosting Multiple Interfaces by co-Doped Graphene Quantum Dots for High Efficiency and Durability Perovskite Solar Cells. *ACS Appl. Mater. Interfaces* 2020, ***12***, 13941–13949. doi:10.1021/acsami.9b23255
137. Shin, S. S.; Lee, S. J.; Seok, S. I. Metal Oxide Charge Transport Layers for Efficient and Stable Perovskite Solar Cells. *Adv. Funct. Mater.* 2019, ***29***, 1900455. doi:10.1002/adfm.201900455
138. Zhu, L.; Shao, Z.; Ye, J.; Zhang, X.; Pan, X.; Dai, S. Mesoporous $BaSnO_3$ Layer Based Perovskite Solar Cells. *Chem. Commun.* 2016, ***52***, 970–973. doi:10.1039/c5cc08156d
139. Bera, A.; Wu, K.; Sheikh, A.; Alarousu, E.; Mohammed, O. F.; Wu, T. Perovskite Oxide $SrTiO_3$ as an Efficient Electron Transporter for Hybrid Perovskite Solar Cells. *J. Phys. Chem. C.* 2014, ***118***, 28494–28501. doi:10.1021/jp509753p
140. Yang, Y.; Liu, Z.; Ng, W. K.; Zhang, L.; Zhang, H.; Meng, X.; Bai, Y.; Xiao, S.; Zhang, T.; Hu, C.; et al. An Ultrathin Ferroelectric Perovskite Oxide Layer for High-Performance Hole Transport Material Free Carbon Based Halide Perovskite Solar Cells. *Adv. Funct. Mater.* 2019, ***29***, 1806506., doi:10.1002/adfm.201806506
141. Acharya, S.; Martha, S.; Sahoo, P. C.; Parida, K. Glimpses of the Modification of Perovskite with Graphene-Analogous Materials in Photocatalytic Applications. *Inorg. Chem. Front.* 2015, ***2***, 807–823. doi:10.1039/C5QI00124B
142. Wang, C.; Tang, Y.; Hu, Y.; Huang, L.; Fu, J.; Jin, J.; Shi, W.; Wang, L.; Yang, W. Graphene/$SrTiO_3$ Nanocomposites Used as an Effective Electron-Transporting Layer for High-Performance Perovskite Solar Cells. *RSC Adv.* 2015, ***5***, 52041–52047. doi:10.1039/C5RA09001F